GA-A15258
UC-77

CORE DESIGN CALCULATIONS FOR MEU FUEL IN FSV

by
M. E. FEHRENBACH and A. M. BAXTER

Prepared under
Contract DE-AT03-76ET35300
for the San Francisco Office
Department of Energy

GENERAL ATOMIC PROJECT 6400
DATE PUBLISHED: OCTOBER 1979

GENERAL ATOMIC COMPANY

ACKNOWLEDGMENTS

The authors wish to thank M. Wan for his help in determining MEU variable self-shielding coefficients. W. Emrich and R. Archibald also contributed considerably to the development and use of the new version of GAUGE used for the physics analysis.

ABSTRACT

Results of a study on the feasibility of converting the Fort St. Vrain reactor core from the present 6-year, High Enriched Uranium (HEU) fuel cycle using uranium enriched to 93% U-235 and Thorium to a 6-year, Medium Enriched Uranium (MEU) fuel cycle using uranium enriched to 20% U-235 and Thorium, are described in this report.

The study shows that a transition from the HEU to MEU cycle can be accomplished, and that operation of the FSV core on a straight MEU cycle is feasible within present Tech. Spec. limits. However, in order to maintain power peaking factors within design limits during the transition cycles when both MEU and HEU fuel are present in the core at the same time, it will be necessary to vary the cycle lengths, use additional burnable poison zoning, change fuel enrichment in several steps from 93% to 20%, or use some combination of these procedures.

CONTENTS

LIST OF TABLES

LIST OF FIGURES

LIST OF FIGURES (cont.)

1. SUMMARY AND CONCLUSIONS

A detailed study was performed of a fuel cycle in the Fort St. Vrain (FSV) core using 20% enriched (20% ε) uranium; the so-called MEU (Medium Enriched Uranium) cycle. Included in this study was a transition from the present high enriched or HEU cycle to an all-MEU cycle on a segment-by-segment reload basis.

This work was an extension of earlier feasibility studies on the use of non-proliferation fuel cycles in the HTGR (1, 2, 3). These studies showed that transition cycles from all HEU to all MEU fuel operating within the constraints on particle design, fuel rod diameter, C/Th ratio and plant operation were feasible for MEU fuel (20% ε) in 3-year semi-annual and 4-year annual cycles, and for 6-year annual fuel cycles at 28% enrichment. Since the 6-year annual fuel cycle is now used for FSV operation, the present work was an attempt at a more detailed investigation of this cycle, using MEU fuel at 20% enrichment, to define more precisely the problems and potential solutions.

Results from this study basically confirm the earlier feasibility work, i.e., for a 6-year cycle at 20% enrichment, maximum region peaking factors exceeded current values at early time points in the first few transition cycles. However, the full equilibrium MEU core has a satisfactory power distribution. Based on the work performed, it is felt that the transition cycle problems can possibly be alleviated by varying fuel cycle length, or by additional burnable poison zoning. Alternatively, the transition to MEU fuel can most easily be accomplished by reducing the enrichment to the 20% level in steps over a 2 or 3 year period. The 20%

enrichment level for uranium has been chosen as a value felt to be most acceptable from a non-proliferation and safeguards standpoint.

2. PHYSICS DESIGN PROCEDURES

The basic FSV core parameters along with the parameters chosen for this design study are summarized in Table 1; particle data in this table was taken from Refs. 4 and 5. A 6-year cycle was chosen to correspond to the current FSV reload interval, along with a U-235 enrichment $\leq$20% to meet non-proliferation concerns. The FSV core layout showing the refueling segment positions is given in Fig. 1.

Many scoping studies have been performed to determine the effects of varying the fuel rod diameter (2). The results indicate that significant gains in reactivity can be obtained if a small fuel rod is used, e.g., 1.1 cm dia. vs. the current FSV value of 1.24 cm dia. This gain is mostly due to the heavy self-shielding in U-238 caused by lumping in the smaller rods. At the time of this study it was also determined that manufacturing problems and costs outweighed any gains due to reactivity effects. The MEU burnup studies were therefore limited to the current FSV fuel rod diameter of 1.24 cm. This cost trade-off should be re-examined in any future design studies.

The first step in the design study was to obtain mass flows for the MEU reloads. Before this could be done, the self-shielding of several nuclides had to be correctly modeled in the nine-group GARGOYLE (6) code used to generate fuel mass flows. A MICROBURN (6) multi-group cross section calculation was made with various uranium and thorium loadings, and self-shielding (g) factors were fitted to the absorption cross sections of the important nuclides as required. All of the g factors were normalized to a particular reference mixture

for which the cross sections were calculated. The reference atom densities of the various nuclides were obtained from scoping studies which optimized the C/Th ratio during the transition cycle, within the constraints of reactivity requirements, fuel rod diameter and particle dimensions.

The choice of a C/Th ratio for any particular reload in the transition cycle was based on reactivity considerations of that particular reload. The Th-232 loading in a reload has a direct impact on that reload as well as several reloads into the future. Since thorium is a neutron absorber that turns into a fuel, it is desirable to load as much as possible in any particular reload, while maintaining sufficient reactivity to operate for a full cycle. It was found that the C/Th ratio in the first few transition cycles had to be increased to ensure that the last transition cycle had sufficient excess reactivity for full operation. This reactivity dip is illustrated in Fig. 20 and discussed later. An alternative procedure, not investigated in detail, would be to vary the length of individual cycles in the transition period while maintaining the total energy output constant over the complete period.

After the determination of the MEU mass flows, the appropriate cross sections were generated for a 2-dimensional burnup calculation with the GAUGE (6) four-group diffusion-theory code. This code was then used to zone the fuel to yield a power distribution that was acceptable from a core performance standpoint, and was stable over the lifetime of the segment. Finally, GAUGE depletion calculations were performed on this zoned fuel over each cycle to yield power distributions, reactivity behavior, and nuclide compositions with time.

3. RESULTS

3.1 Cross Sections

The generation of suitably self-shielded multi-group cross sections proved more difficult for MEU than for the HEU fuel because of the increased importance of the nuclides U-238, Pu-239, and Pu-240, which have complex resonance structures. In particular, the importance of U-238 in the MEU calculations made it necessary to develop a set of shielding coefficients for the energy groups encompassing the large U-238 resonances. For this case, the problem is also complicated by the fact that during the six year transition period, the core contains both HEU and MEU fuel with differing spectra and shielding requirements.

The major problem lies in providing concentration dependent g factors which reflect the change in resonance cross section behavior with nuclide burnup; in this regard, a study was performed on the variations that the cross sections of the major nuclides U-235, U-238, Th-232 and Pu-239 undergo during in-core life. It was found that the time dependence of the g factors for the important resonance absorbers, e.g., U-238 and Th-232, was best represented as a function of their own density, while nuclides such as U-235 were best fit to $\Sigma_{a_{rod}}$ (macroscopic absorption cross section in the rod). Figures 2, 3 and 4 illustrate this effect for the thermal group absorption cross section for U-235. (The neutron energy group structure used in the burnup calculations is given in Table 2). Figure 2 shows that the time dependence of the g factor (i.e., its variation with burnup) correlates well with the total thermal group macroscopic cross section (essentially

$\Sigma_{a_4}^{233} + \Sigma_{a_4}^{235}$), but fits rather poorly to Σ_a^{235} or to the U-235 atom density (N-235) alone as in Fig. 3 and 4. The two fissile uranium isotopes comprise about 70% of the thermal fission cross section in most of the cases studied. The effects of Pu-239 become more important with burnup, but if the U-235 g factor is computed using a U-235 shielding set fitted to $\Sigma_{a_{rod}}$, it will be consistent with most loadings throughout the core. Several other curve fits were tried for U-235, but none were acceptable over the range of loadings necessary for optimum fuel zoning. Figures 4 through 6 show results of various attempts at fitting the U-235 thermal cross section to other possible correlating factors. As can be seen, the fits are not as good as for the total thermal group absorption cross section. Figures 7 and 8 show the effect of thorium loading on the U-238 cross section variation with burnup. Most of the effect occurs in the resonance region (group 2 of group 4, group 4 being the thermal group), where the Th-232 cross section is a significant fraction of the group cross section. The effect is seen in Fig. 7 as a spreading of the data points. Figure 8 also shows that Σ^3_a rod increases with burnup while the other groups decrease. This is probably due to a significant U-233 cross section in this energy group.

The behavior of the Pu-240 cross section with burnup is also very complex as shown in Fig. 9. Fortunately, its effects were not large in this design study so that self-shielding for this nuclide could be safely neglected.

Based on these studies "best-fit" curves were determined for the important resonance cross section nuclides over the wide range of loading changes to be encountered in the FSV design study. These g-factor curve fits for Th-232, U-235, and U-238 are shown in Figs. 10 through 15 for the 9-group cross section set used in the GARGOYLE zero-dimensional studies, and in Figs. 16 through 19 for the 4-group cross section set used in the GAUGE two-dimensional burnup analysis. The corresponding coefficients are listed in Tables 3 and 4.

In Fig. 18, the case labeled "DRIVER" refers to an all uranium driver block. The plot shows the effect of Th-232 on the U-238 cross section in group 2. This effect is absent in group 3, where the Th-232 cross section is insignificant (see Fig. 19). The effect of Th-232 on the U-238 cross section is important if the MEU/Th-MEU/DRIVER core is ever utilized. (In this concept the thorium is restricted to sufficiently few fuel blocks that the C/Th ratio in these blocks corresponds to that in HEU fuel. U only fuel is used in the rest of the blocks in a segment. This concept would provide a reasonable test for fuel recycle.) Use of these fits permitted rapid evaluation of various loading schemes and accurate burnup analysis for the FSV design studies.

3.2 Reactivity Considerations

The feed searches using these cross section sets were performed with the 9-group (Table 2), zero-dimensional, diffusion theory code GARGOYLE. An end-of-cycle reactivity of $k_{eff} = 1.015$ was assumed for these feed searches to allow for uncertainties in the calculational model and basic data sets. All cases assumed 20% enriched uranium feed. The first feed searches with the reference fissile loading indicated that an equilibrium C/Th ratio of >3000 (Fg. 20) would produce the desired reactivity behavior. This C/Th ratio is about a factor of 15 over the HEU C/Th ratio in FSV.

3.3. Power Distributions

Besides end-of-cycle (EOC) reactivity, an additional constraint on these zero-dimensional feed searches is the Age Peaking Factor (APF). This is the ratio of the macroscopic fission cross section in the fresh fuel to the core average value; and is directly related to the maximum region peaking factors (RPF) and hence fuel temperatures that can be expected from the more detailed dimensional burnup calculations (e.g., with the GAUGE code). From previous HEU analyses, a limit on

APF of approximately 1.4 had been found necessary to ensure acceptable RPFs in the detailed dimensional studies. Although a similar detailed correlation has not been completed for MEU fuel, preliminary results indicate that a similar limit should also hold, thus the 1.4 APF limit was assumed in the present work.

In HEU cores, thorium is the main absorber present and thus C/Th can be simply correlated with EOC reactivity and with power distributions through the APF. For MEU fuel, however, the additional U-238 introduces an extra free variable; and complicates the process of determining a satisfactory loading combination which simultaneously meets reactivity constraints, power peaking limits, and maximizes thorium loading. This problem has been discussed elsewhere (see Ref. 2). For the present case, an iterative procedure was used with the GARGOYLE code to determine the optimum loadings. The maximum allowable APF was fixed and the uranium load or C/U ratio to produce the desired EOC reactivity at equilibrium conditions was determined. A series of cases was then run with varying thorium loadings, within the constraints of allowable packing fractions, to evaluate performance during the transition cycles. Figures 20, through 22 summarize the results of these studies, while Fig. 23 shows the behavior of the best C/U and C/Th combinations. Figures 24 illustrates the relationship between C/U and C/Th ratios in the equilibrium MEU core and shows that any increase in thorium loading beyond that used in the Survey studies requires a significant uranium loading increase.

It was decided to approach equilibrium as rapidly possible, but within these age peaking constraints. Figure 25 demonstrates the effects of different age peaking constraints on the transition cycle. At a constant 20% uranium enrichment, it was necessary to exceed the 1.4 APF in order to achieve acceptable EOL reactivity levels through the six year transition from HEU to MEU fuel. The 1.4 limit places a severe restriction on the amount of Th-232 loaded each year and the reduced production of U-233 causes reactivity problems in the sixth

cycle. Alternatives not pursued in this study include: varying cycle lengths while maintaining total energy production, decreasing U-235 enrichment in steps, or removing Th-232 completely from some blocks in each segment. Full equilibrium MEU studies indicate that the age peaking will be below 1.3 so that no power peaking problems will be encountered once the transition is made.

Tables 5 and 6 give the loadings from GARGOYLE feed searches with age peaking limits of 1.50 and 1.55, respectively. The 1.50 case was chosen, although the 1.55 case approaches equilibrium much faster, because it was felt that an age peaking of 1.55 would be too high to meet core performance limitations.

Several modifications had to be made to the GAUGE code to properly model MEU fuel. The large amount of U-238 in the core as compared to HEU cycles made it necessary to have several shielding options. In particular, region dependent shielding was necessary because of the differences between MEU and HEU fuel, present at the same time in the core and two dimensional shielding tables were also required to handle the wide variation in MEU g factors. Rational functions of the type $(C_1 + C_2\ \Sigma + C_3\ \Sigma^2)^{-1}$, used for all previous HEU studies, cannot handle this wide variation, and, in addition, this procedure leads to discontinuities at the roots of the second order polynomial. Figure 26 is a plot demonstrating the behavior of the rational self-shielding formula for Th-232 (group 3) in the MEU fuel. In most normal applications the curve fit covers the desired range of number densities; however, in most instances 2-D tables will give more accuracy over a larger range.

In addition to the transition cycles, the study was extended to include the FSV core with a full equilibrium MEU fuel cycle. The first MEU equilibrium cycle (core reload 18, MEU segment 13) had to be zoned somewhat differently from the corresponding HEU core. The fissile zoning ratio used was 1:1:0.65 for the inner, outer, and buffer regions,

respectively; and the Th-232 loading in the buffer blocks was increased to compensate for the reduced U-235 loading. MEU fuel burns out faster than HEU fuel and therefore requires a higher BOC U-235 loading in the newly refueled regions. Due to the higher initial U-235 loading, the new segments require almost double the burnable poison loading of HEU segments to achieve acceptable reactivity behavior during the cycle and suitable power distribution in the fresh fuel.

The equilibrium cycle power distributions are within the FSV Tech. Spec. limits as shown in Table 7. The highest region peaking factors occur during the first few days of each reload and burn down rapidly. The use of burnable poison wafer between fuel rods in an element rather than rods of B_4C at the corners of an element will allow greater flexibility in the poison zoning and a corresponding improvement in power distribution and reactivity control. Poison wafers, which consist of carbon coated B_4C particles in a graphite matrix have been specified for the large HTGR core designs.

Table 8 summarizes the equilibrium fuel loadings. The equilibrium C/Th ratio in fresh segments is about 875, and the corresponding C/U ratio is 400.

Figures 20-23 all demonstrate the large reactivity dip that is observed when the HEU segments are replaced by MEU fuel. It is this decrease in reactivity that makes it necessary to load a large amount of U-235 and a small amount of Th-232 in these segments. This requirement in turn creates a low conversion ratio in these segments and they burn out faster than desired. When a new segment is loaded, there is a large difference in reactivity between the new fuel and the old fuel resulting in high RPF's. Burnable poison control can reduce these RPF's somewhat, but LBP cannot be made to burn out any faster than in the homogenous case. Even with homogenous burnable poison control, it will be difficult to achieve an acceptable power distribution in the transition cycle. Figures 27 and 28 depict typical RPF distribution for the transition cycle and

equilibrium cycles respectively. The MEU transition cores are also restricted by high tilts which are a direct consequence of not having enough Th-232 in the core for power stability. Tilts exceeding 1.6 in the outer core regions were typical in the transition cycle, and tilts of 1.7 were not uncommon.

REFERENCES

1. Asmussen, K. E., and J. T. Ganley, "Core Design and Feasibility Study for LEU and MEU/Th-Fueled HTGRs", General Atomic Report GA-A14757, June 1978.

2. Merrill, M. H., and R. K. Lane, "Medium-Enriched Uranium/Thorium Fuel Cycle Parametric Studies for the HTGR", General Atomic Report GA-A14659, December 1977.

3. Asmussen, K. E., A. M. Baxter, et al., "Low-Enrichment and Denatured (Thorium) Fuels for the HTGR: A Status Report", General Atomic Report, GA-A14606.

4. Smith, C. L., "Design Memo MDD-FSV-012-77; TRISO UC_2 and TRISO ThO_2 Fuel Performance Models for FSV", Doc. No. MDD-FSV-012-77, December 1977.

5. Smith, C. L., "Design Memo MDD-FSV-011-77; Failure Criterion, Kernel Migration in FSV", Doc. No. MDD-FSV-011-77, December 20, 1977.

6. Merrill, M. H., "Nuclear Design Methods in Use at Gulf General Atomic", General Atomic Report GA-A12652, July 1973.

TABLE 1

PARAMETERS USED FOR MEU/Th FSV CORE DESIGN STUDIES

a) Basic FSV Core Parameters

Thermal Power	842 MW(t)
Effective Core Diameter	594.4 cms (19.5 ft)
Active Core Height	475.5 cms (15.6 ft)
Number of Fuel Elements	1482
Number of Fuel Columns	247
Reflector Thickness (average)	118.9 cms (3.9 ft)
Number of Refueling Regions	37
Number of Control Rods	37 pairs
Fuel Lifetime	6 years
Fraction of Core Replaced Each Year	∿1/6
Fuel Cycle	Uranium/Thorium

b) MEU Reload Segment Parameters

Fuel Cycle Length (years)	6
U-235 Enrichment (%)	≤20
Fuel Rod Diameter, d (cms)	1.27
C/Th	See Text

Particle Data	Dimension	Density
Fissile		
Kernel (UCO)	350μ diam.	10.5 gm/cc
Buffer	110μ thick	1.05 "
IPyC	35μ "	1.90 "
SiC	35μ "	3.20 "
OPyC	45μ "	1.80 "
Total Particle	800μ diam.	
t/d	0.643	
Fertile		
Kernel (ThO_2)	450μ diam.	9.9 gm/cc
Buffer	60μ thick	1.05 "
IPyC	35μ "	1.9 "
SiC	35μ "	3.2 "
OPyC	45μ "	1.8 "
Total Particle	800μ diam.	
t/d	0.389	

TABLE 2

NEUTRON ENERGY GROUP STRUCTURE USED IN BURNUP CALCULATIONS

Group Lower Boundary (ev)

		9 Group GARGOYLE		4 Group GAUGE
FAST	1)	1.83×10^5	1)	1.83×10^5
	2)	961	2)	17.6
	3)	17.6	3)	2.38
	4)	3.93		
	5)	2.38		
THERMAL	6)	0.414	4)	0.0
	7)	0.10		
	8)	0.04		
	9)	0.0		

TABLE 3

VARIABLE SELF-SHIELDING COEFFS. FOR 9 GROUP GARGOYLE* CALCULATIONS

Nuclide/group	C_1	C_2	C_3
Th-232/3	1.2795	401.68	-66,548.
U-238/3	1.9018	698.70	-68,442.
U-238/4	1.9719	318.73	-11,601.
U-235/7	1.0301	18.461	-2,191.1
U-235/8	1.0505	8.3763	-382.26
U-235/9	1.1068	8.9317	-200.53

(Fuel Rod Dia = 1.2446 cm)

*GARGOYLE self-shielding formula:

$$g = C_1/(1 + C_2 \Sigma + C_3 \Sigma^2)$$

TABLE 4

SELF-SHIELDING COEFFICIENTS* USED IN 4 GROUP GAUGE BURNUP STUDIES

Nuclide	Group	C_1	C_2	C_3
Th-232	2	0.8524	280.63	528661.0
U-238	2	0.5116	885.54	-179660.0
U-238	3	0.5425	195.14	-7848.2

*GAUGE self-shielding formula:

$$g = (C_1 + C_2 \Sigma + C_3 \Sigma^2)^{-1}$$

Group	Energy Range (eV)
1	∞ - 1.83+5
2	1.83+5 - 17.6
3	17.6 - 2.38
4	2.38 - 0

TABLE 5

RESULTS OF FEED SEARCH FOR MEU TRANSITION CYCLES IN FSV

WITH MAXIMUM APF LIMIT ∿1.5

MEU Cycle	Age Peaking	Kg U-235	Kg Th-232	EOC K_{eff}	Loaded C/Th
1	1.507	204.2	913.9	1.015	580
2	1.495	210.3	488.0	1.015	1082
3	1.486	218.8	370.8	1.015	1424
4	1.489	230.0	180.8	1.017	2915
5	1.475	237.7	63.3	1.018	8392
6	1.453	242.4	0	1.015	--
7	1.443	245.9	586.4	↑	900
8	1.427	250.6	396.6	↑	1333
9	1.403	254.4	367.8	↑	1434
10	1.355	↑	307.8	↑	1715
11	1.307	↑	256.0	↑	2063
12	1.262	↑	223.0	↑	2785
13	1.249	↑	582.9	↑	907
14	1.235	↑	500.0	↑	1056
15	1.223	↑	493.3	↑	1071
16	1.210	↑	442.8	↑	1192
17	1.195	↓	395.0	↓	1335
18	1.180	254.4	383.8	1.015	1451

TABLE 6

RESULTS OF FEED SEARCH FOR MEU TRANSITION CYCLES IN FSV

WITH MAXIMUM APF LIMITS OF 1.55

MEU Cycle	Age Peaking	Kg U-235	Kg Th-232	EOC K_{eff}	Loaded C/Th
1	1.55	211.9	989.3	1.015	535
2	1.546	223.0	584.9	1.015	903
3	1.542	238.1	484.7	1.015	1089
4	1.529	254.4	218.5	1.018	2416
5	1.439	↓	57.8	1.019	9132
6	1.373	↓	0.0	1.015	--
7	1.340	↓	635.7	↓	830
8	1.309	↓	464.7	↓	1137
9	1.287	↓	484.7	↓	1089
10	1.264	↓	418.1	↓	1262

TABLE 7

EQUILIBRIUM CYCLE

Max. RPF	Time in Cycle
1.40	2
1.39	5
1.45	10
1.42	50
1.46	100
1.51	150
1.45	200
1.50	250
1.47	292

TABLE 8

TYPICAL FUEL MASS FLOW DATA FOR AN MEU EQUILIBRIUM CYCLE (Reload 18) IN THE FSV CORE

Nuclide	Kg Loaded	Kg Discharged
Th-232	573.1	526.8
U-234	1.6	0.8
U-235	254.4	58.6
U-238	1030.5	906.9
Pu-239	--	18.6
U-233	--	21.8*
LPP	0.84	--

* Sum of Pa-233 and U-233 in discharged fuel

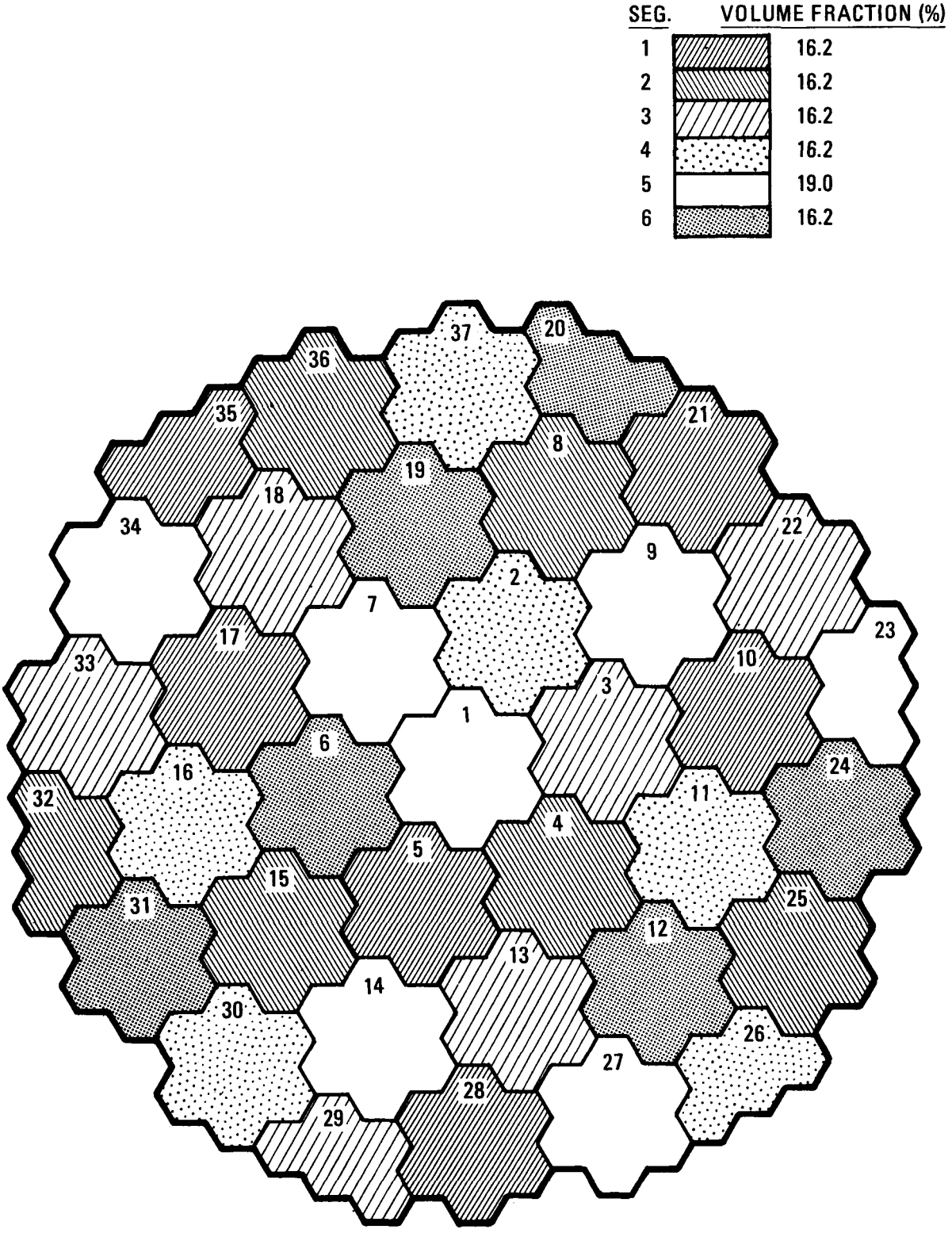

Fig. 1 FSV 6-year cycle core layout

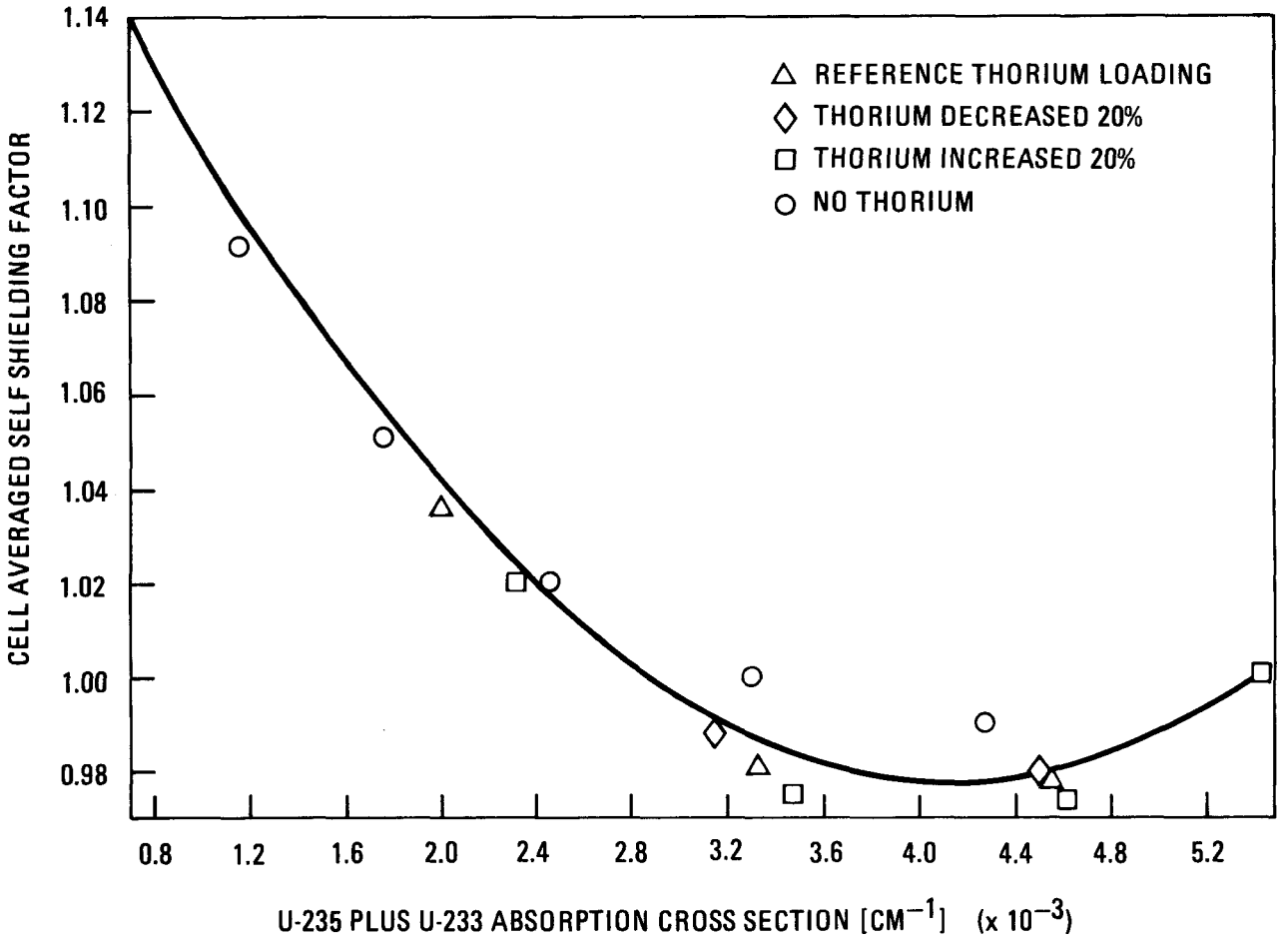

Fig. 2 U-235 thermal group self-shielding factor for various Th-232 loadings

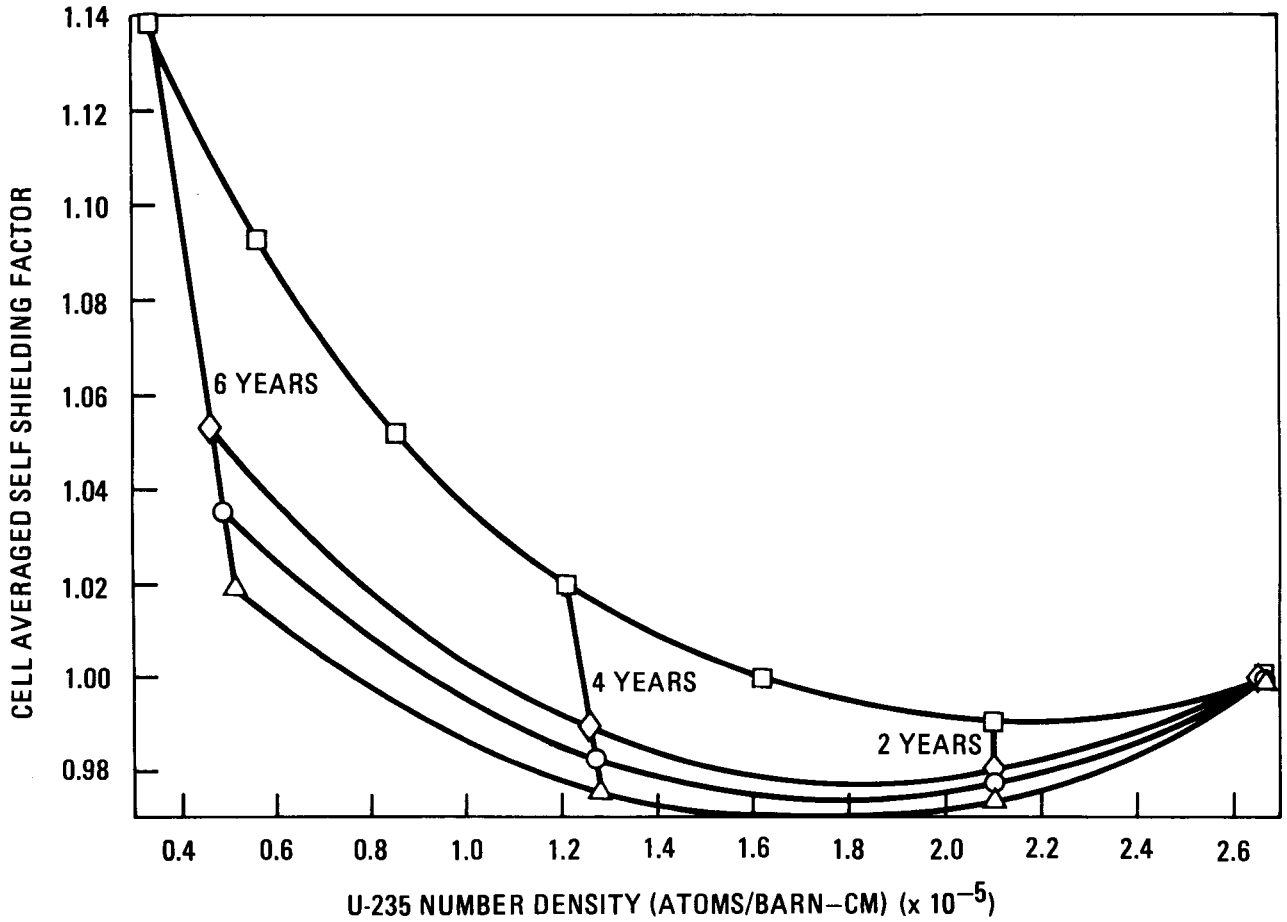

Fig. 3 U-235 self-shielding factor vs. atom density for various Th-232 loadings

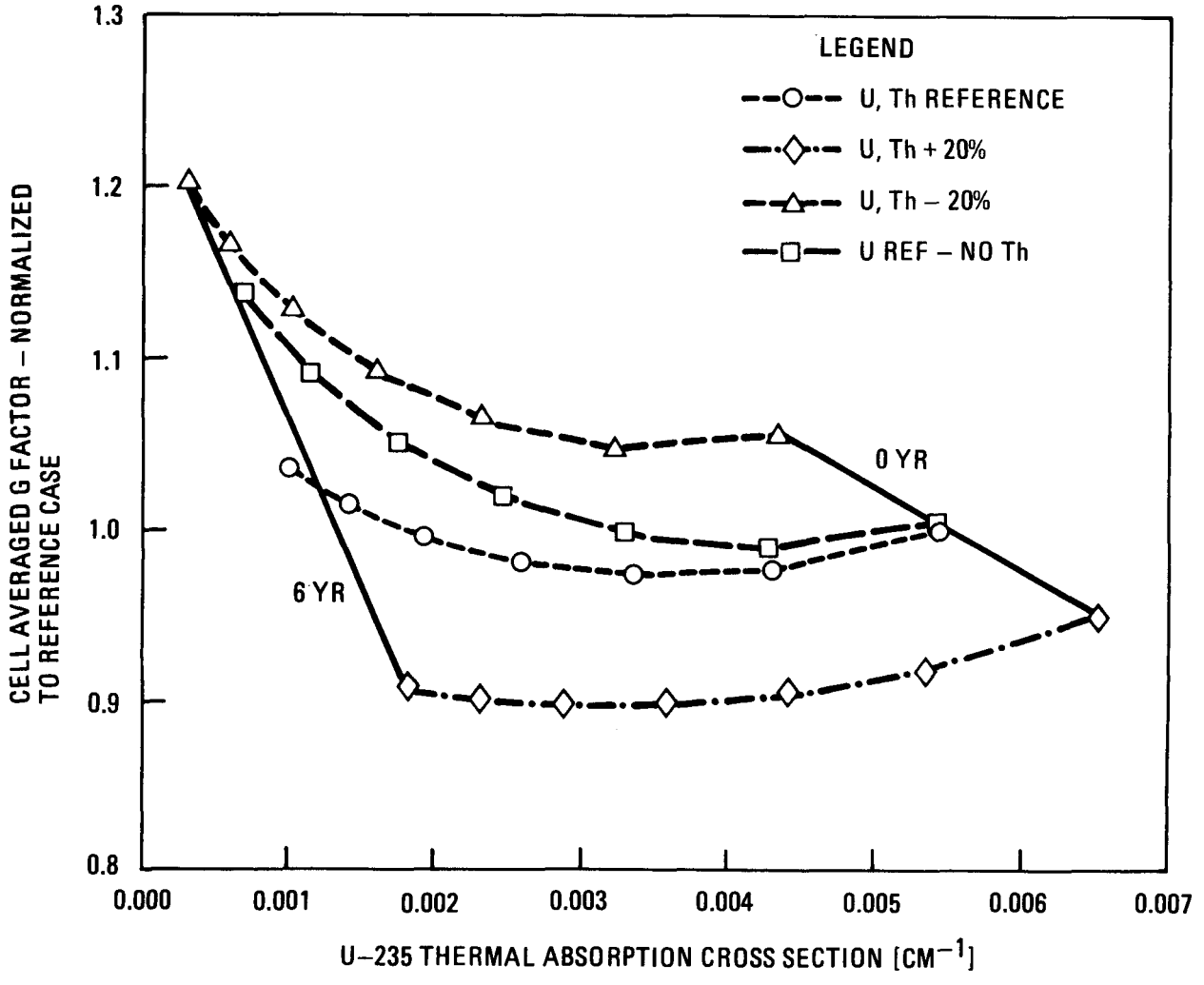

Fig. 4 Change in U-235 shielding factor as a function of U-238 thermal absorption cross section

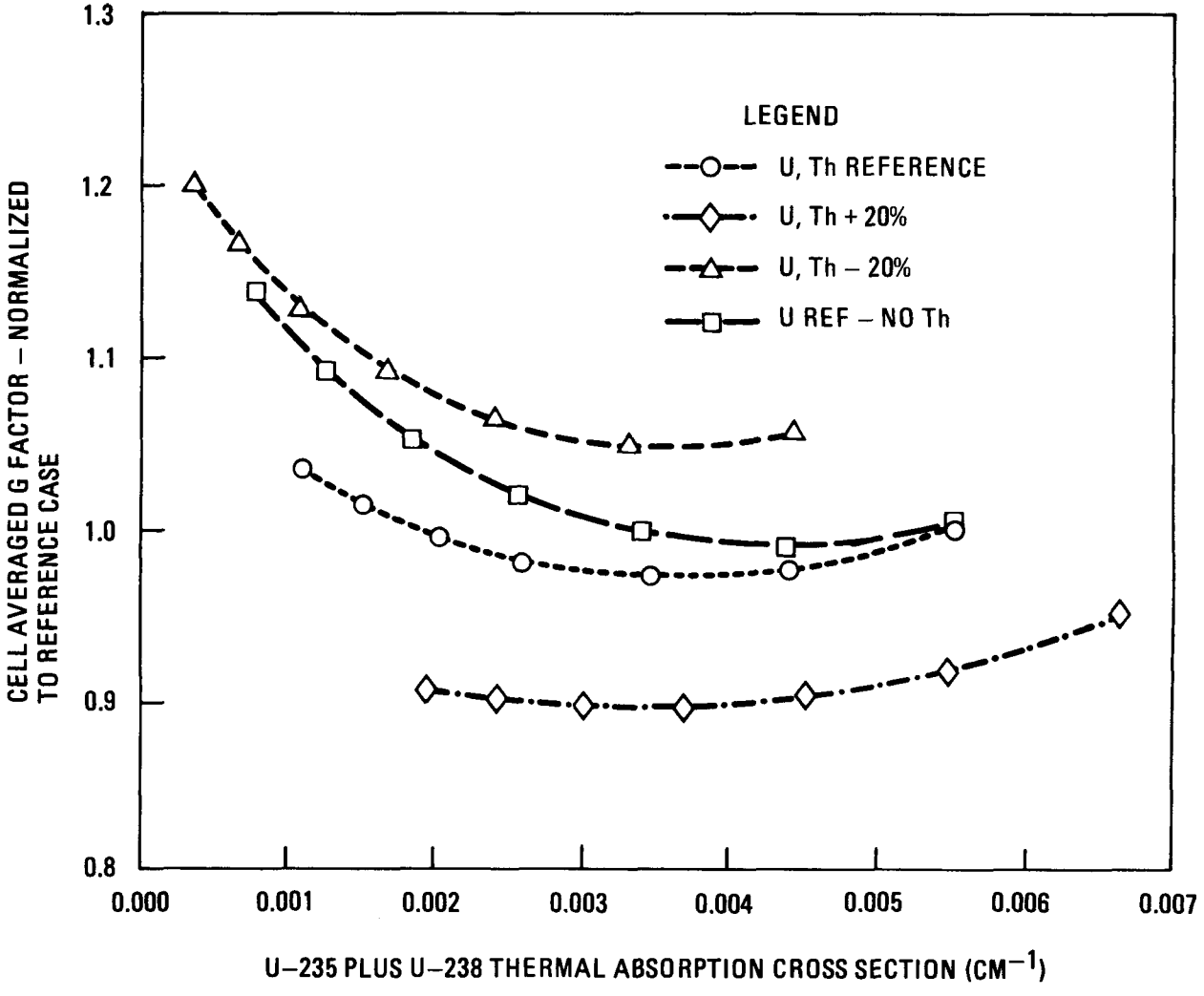

Fig. 5 Variation of U-235 g factor as a function of U-235 plus U-238 thermal absorption cross section

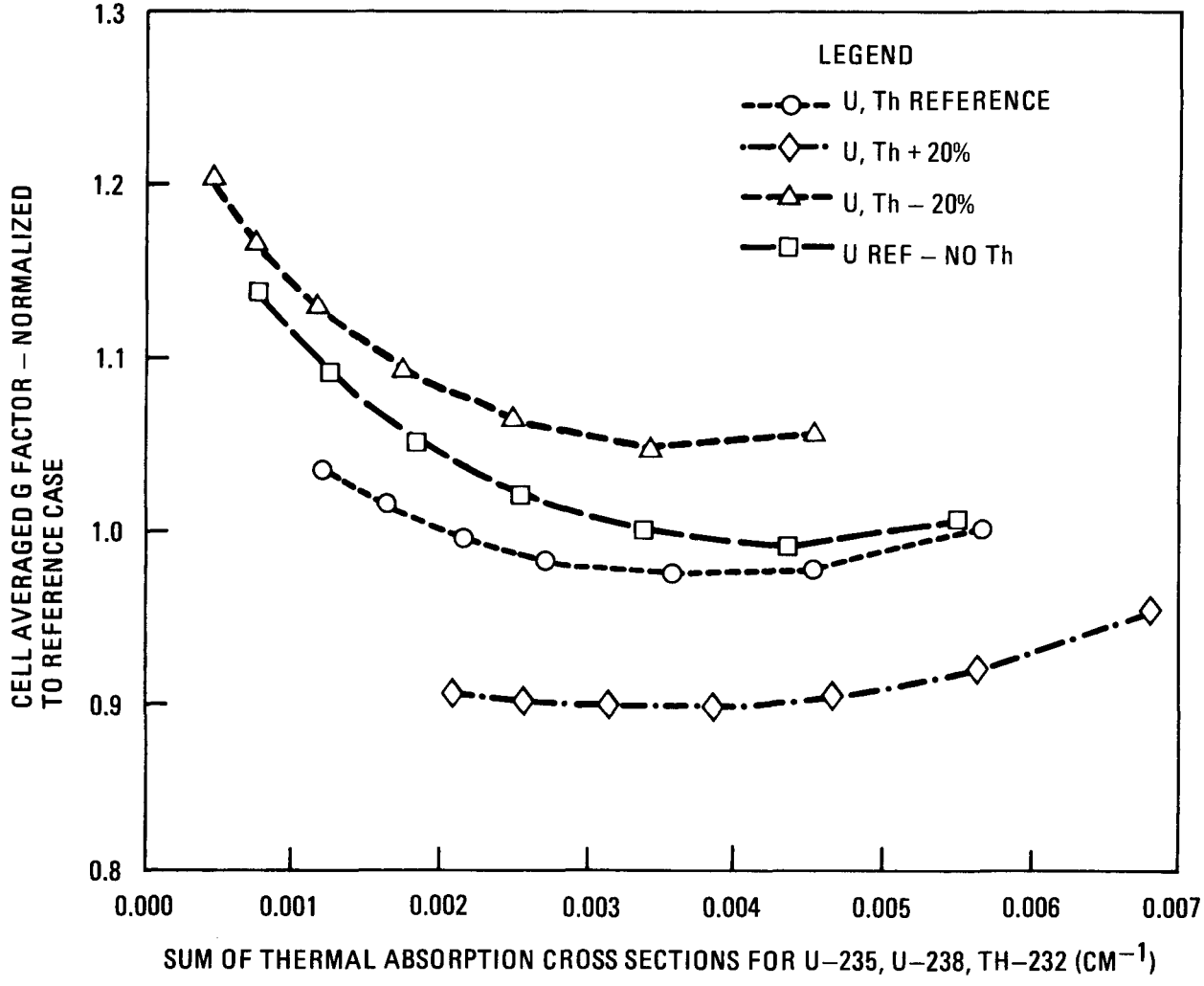

Fig. 6 Variation of U-235 g factor as a function of U-235 plus U-238 plus Th-232 thermal absorption cross section

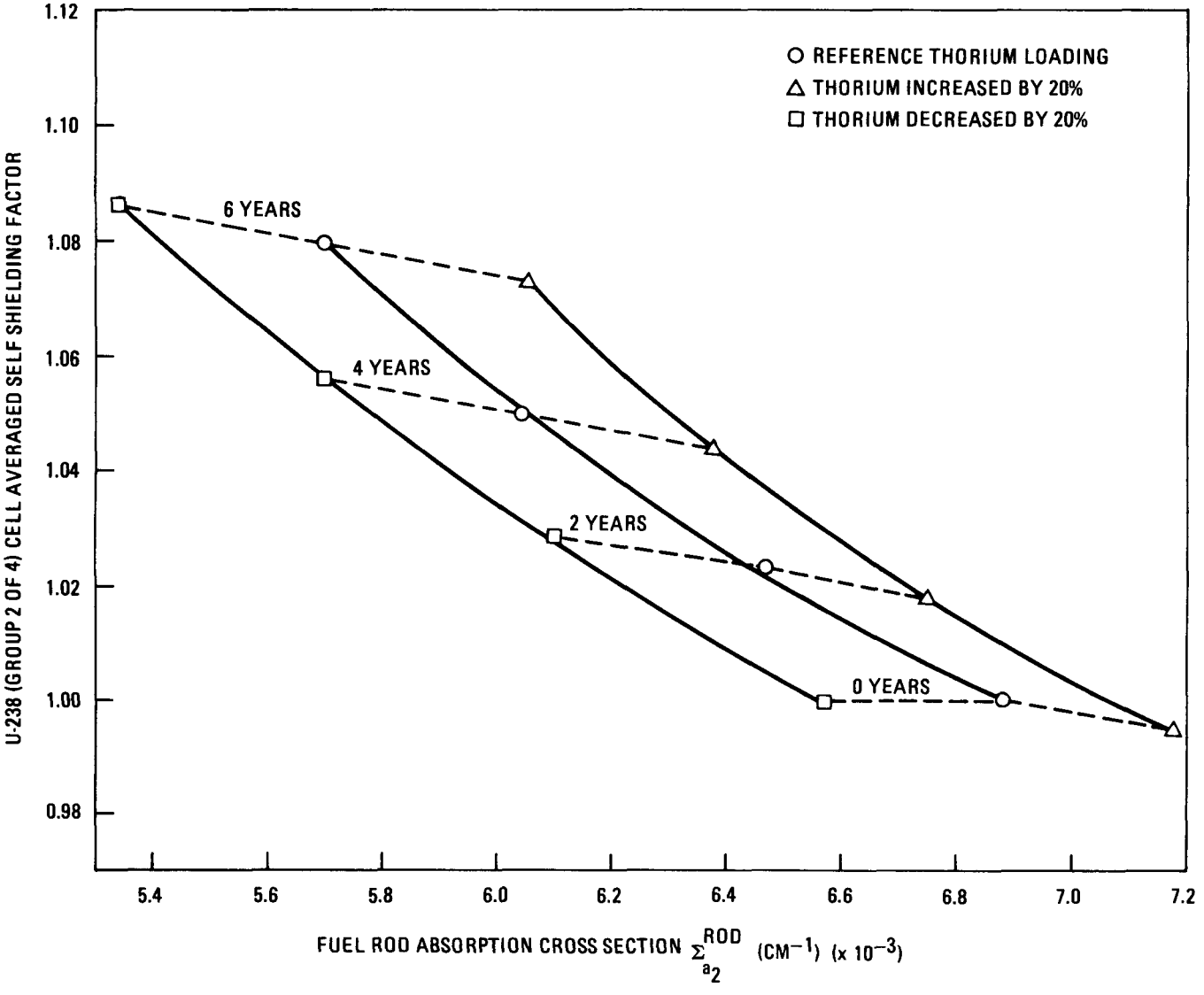

Fig. 7 Effect of thorium loading on U-238 g factor - Group 2

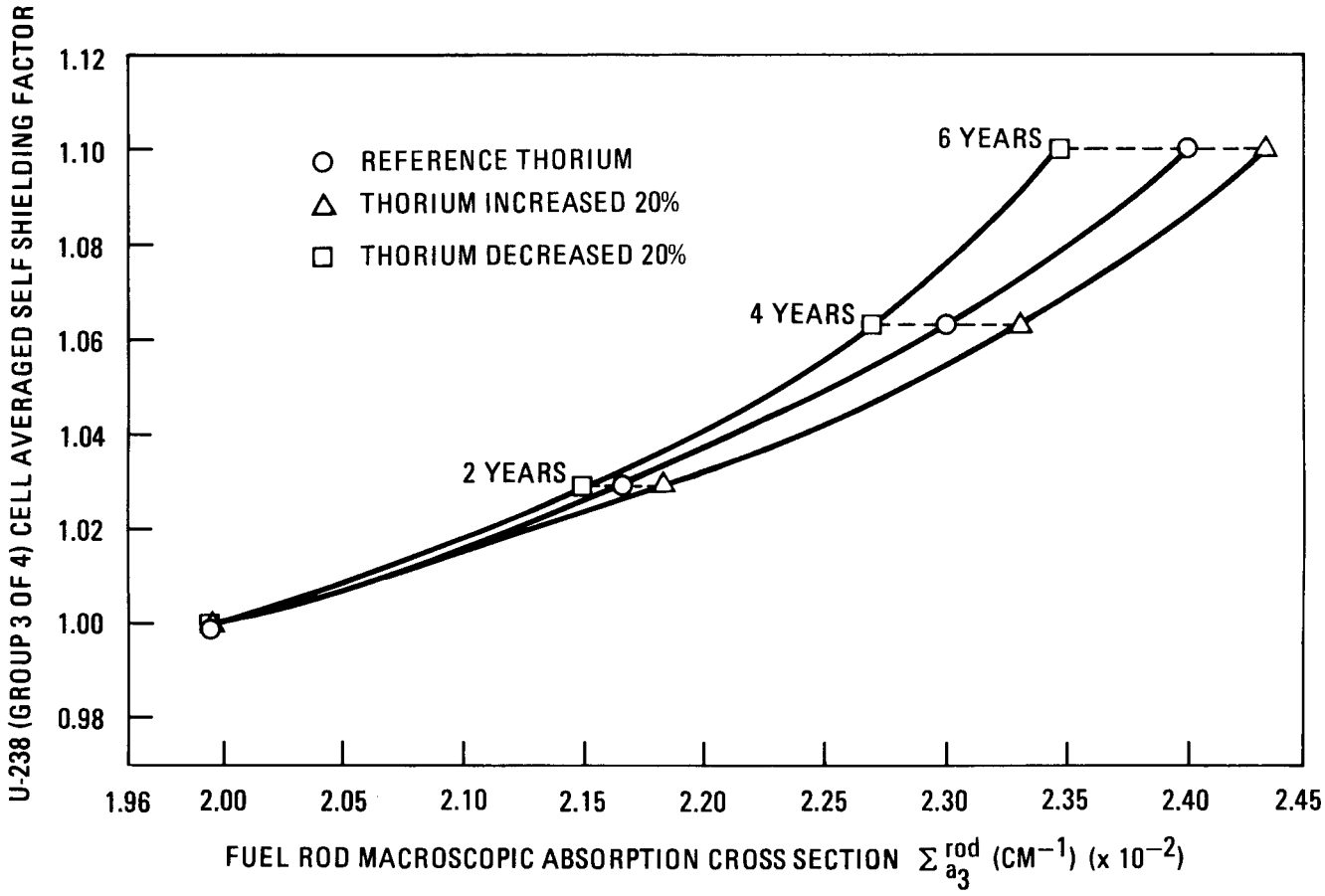

Fig. 8 Effect of thorium loading on U-238 g factor - Group 3

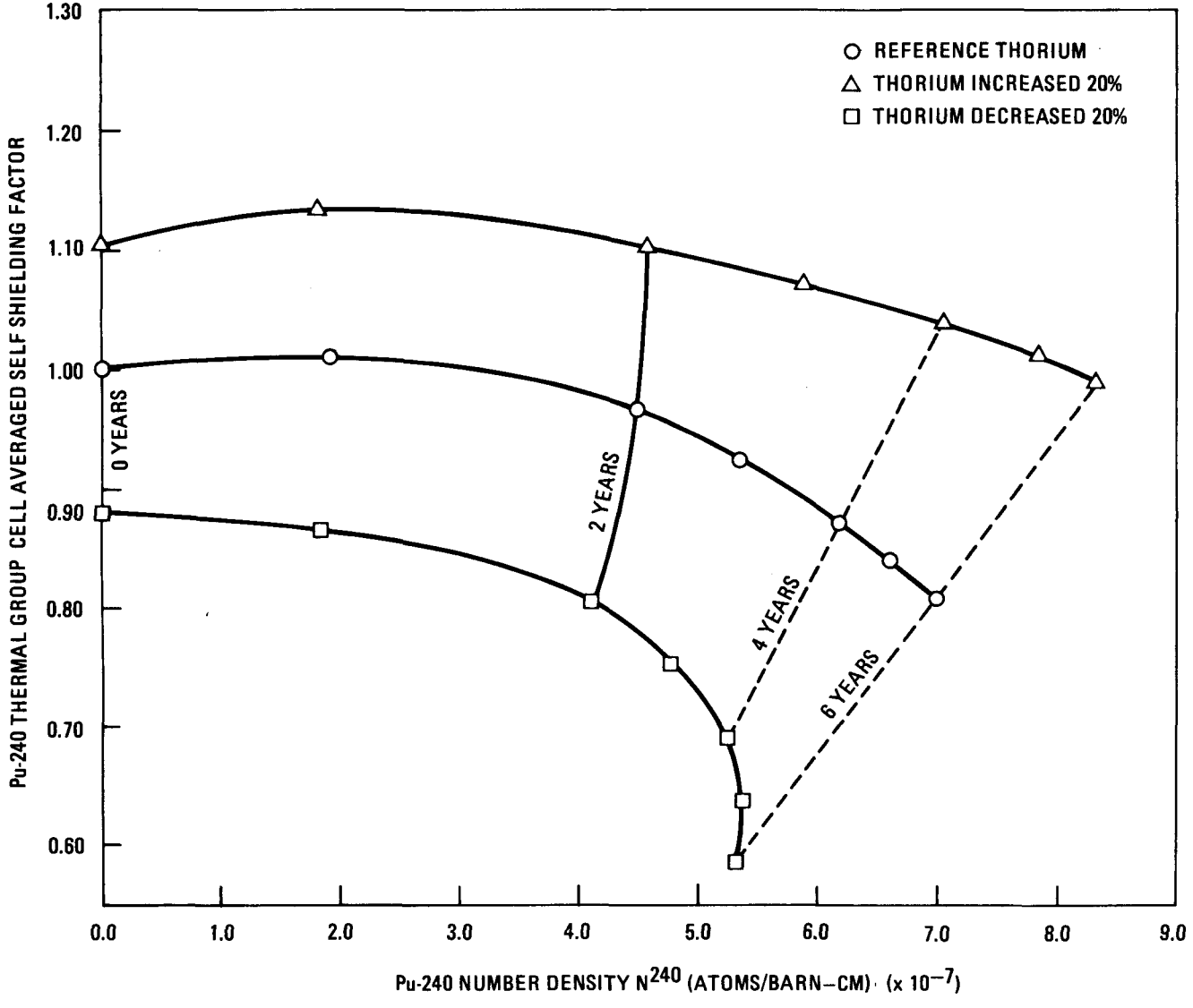

Fig. 9 Behavior of Pu-240 g factor with burnup and thorium loading changes

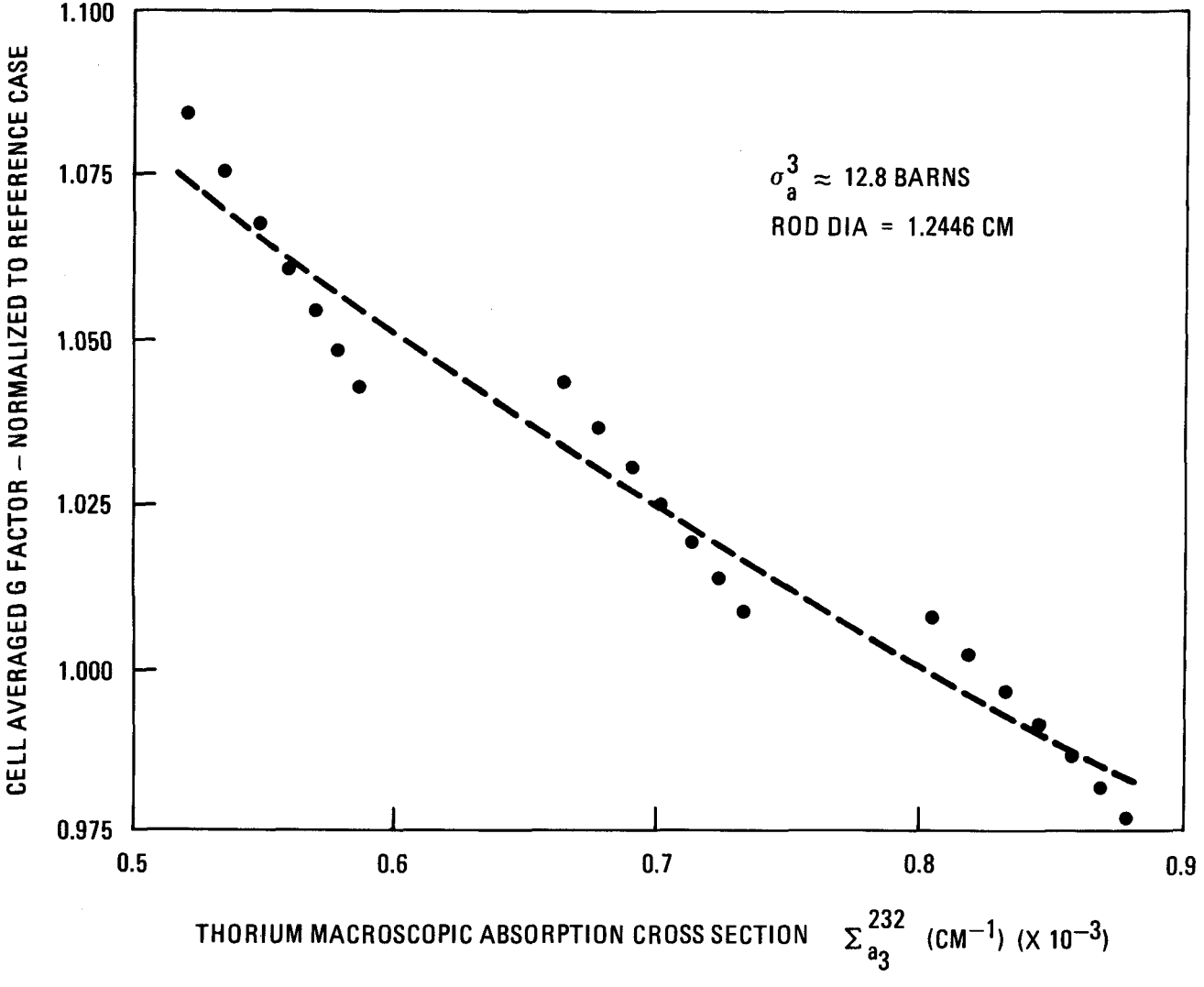

Fig. 10 Thorium self-shielding factor - GARGOYLE Group 3

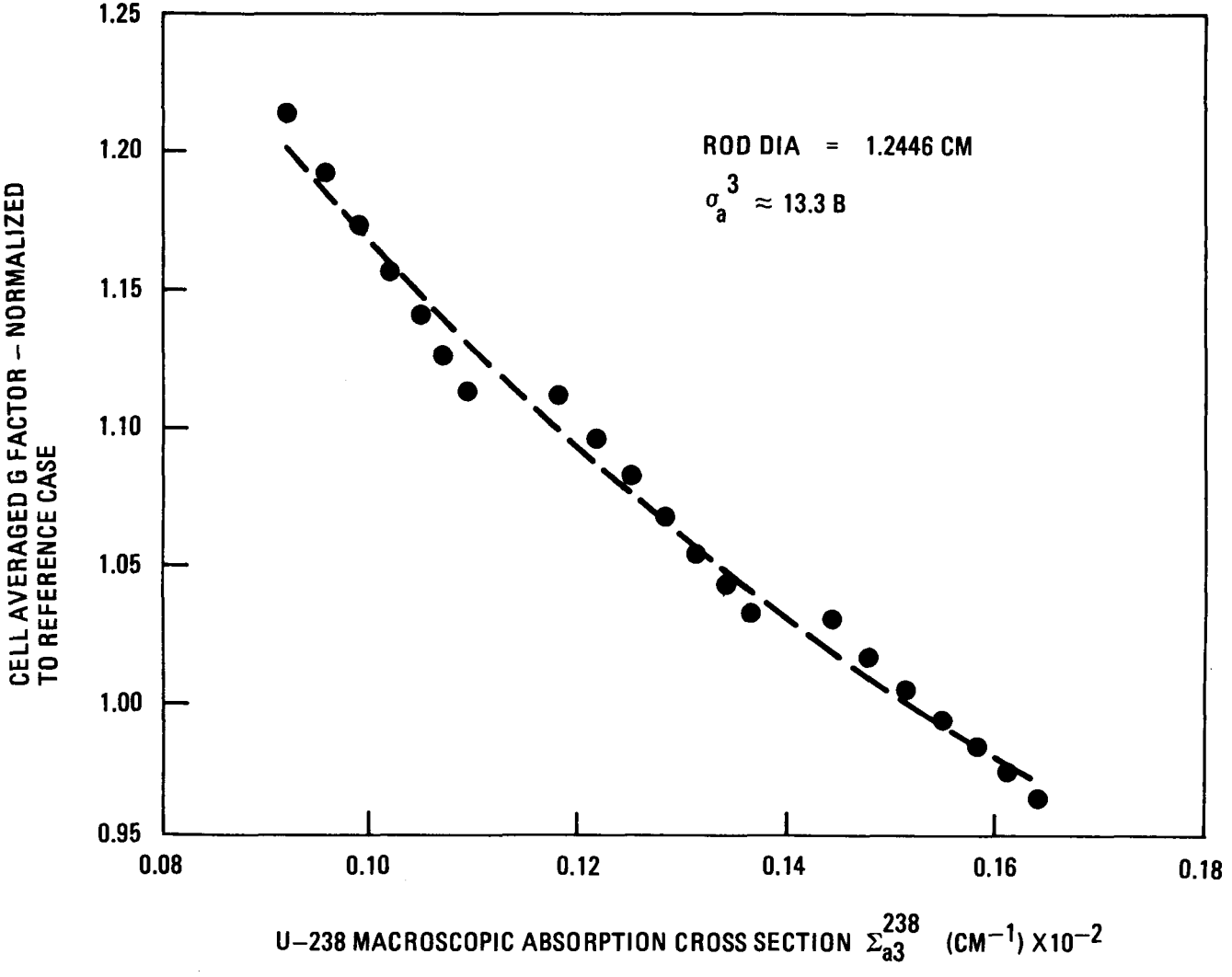

Fig. 11 U-238 self-shielding factor - GARGOYLE Group 3

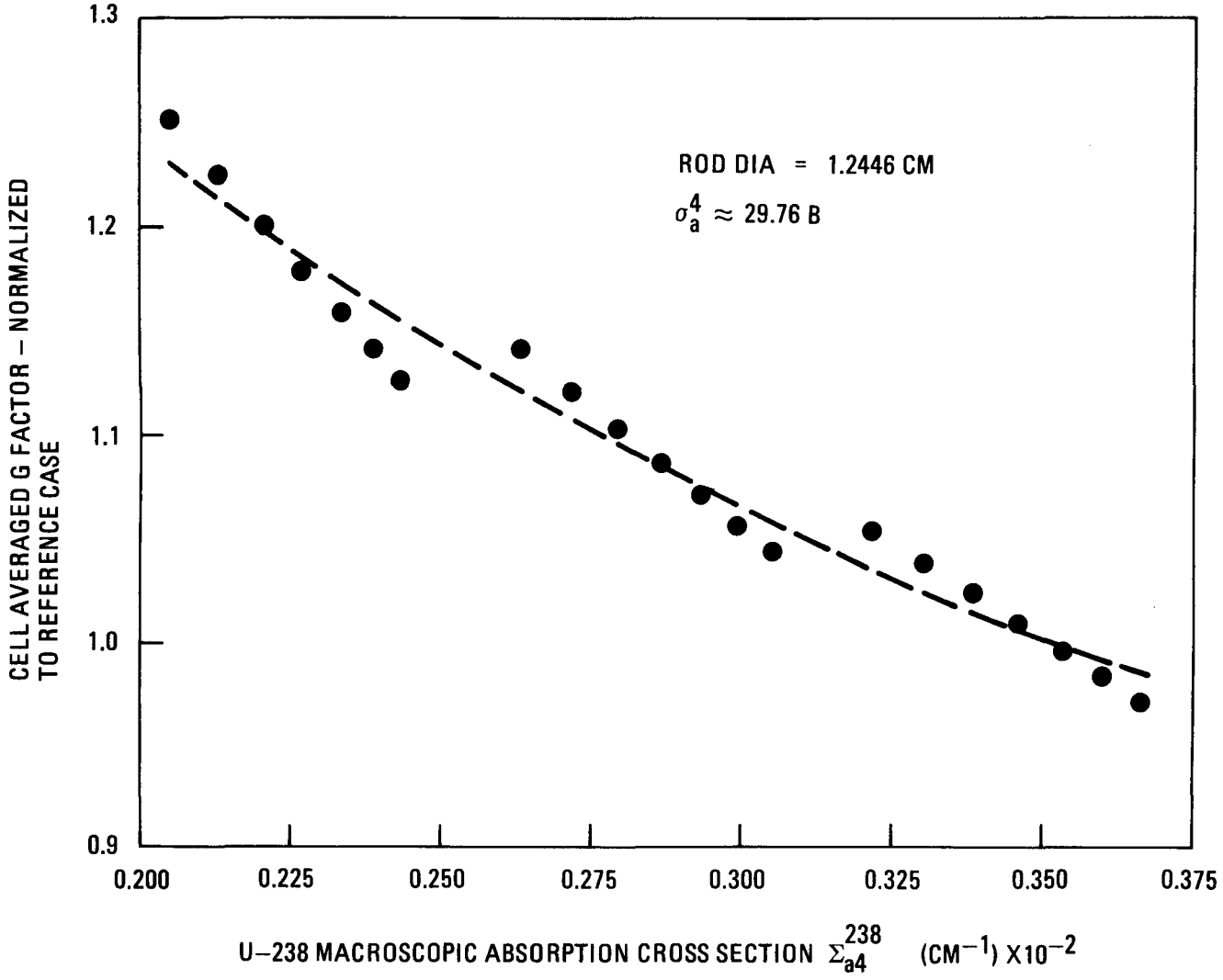

Fig. 12 U-238 self-shielding factor - GARGOYLE Group 4

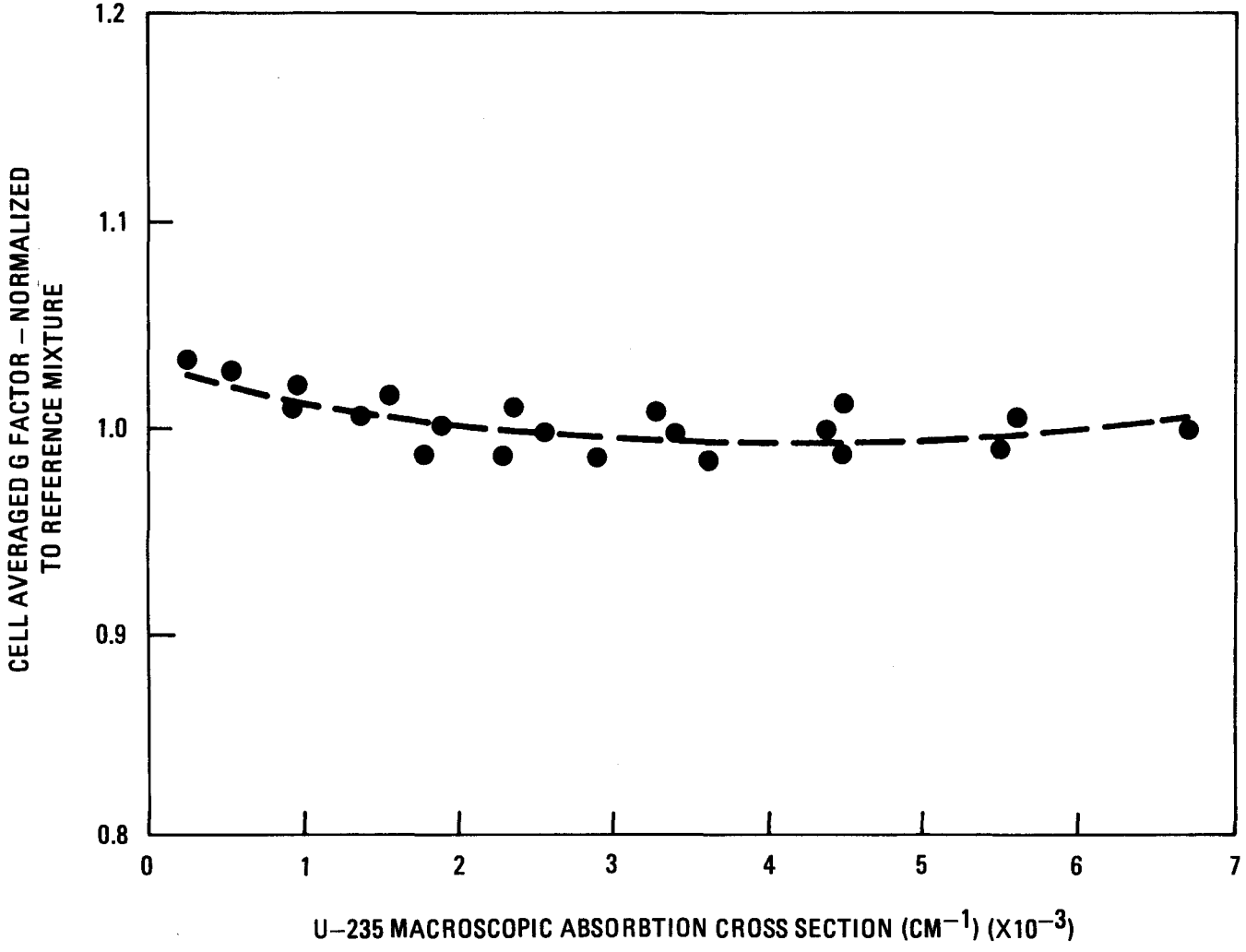

Fig. 13 U-235 self-shielding factor - GARGOYLE Group 7

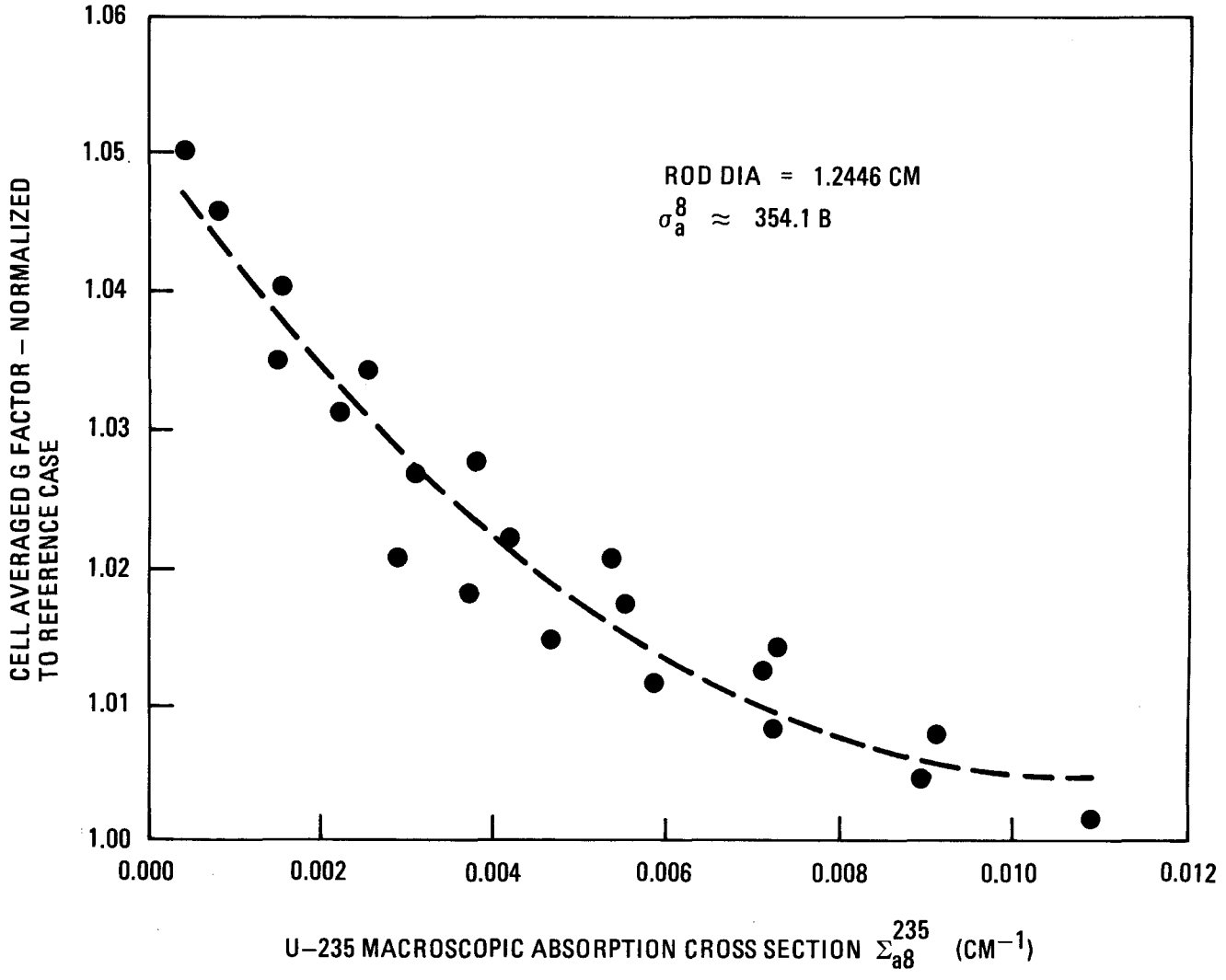

Fig. 14 U-235 self-shielding factor - GARGOYLE Group 8

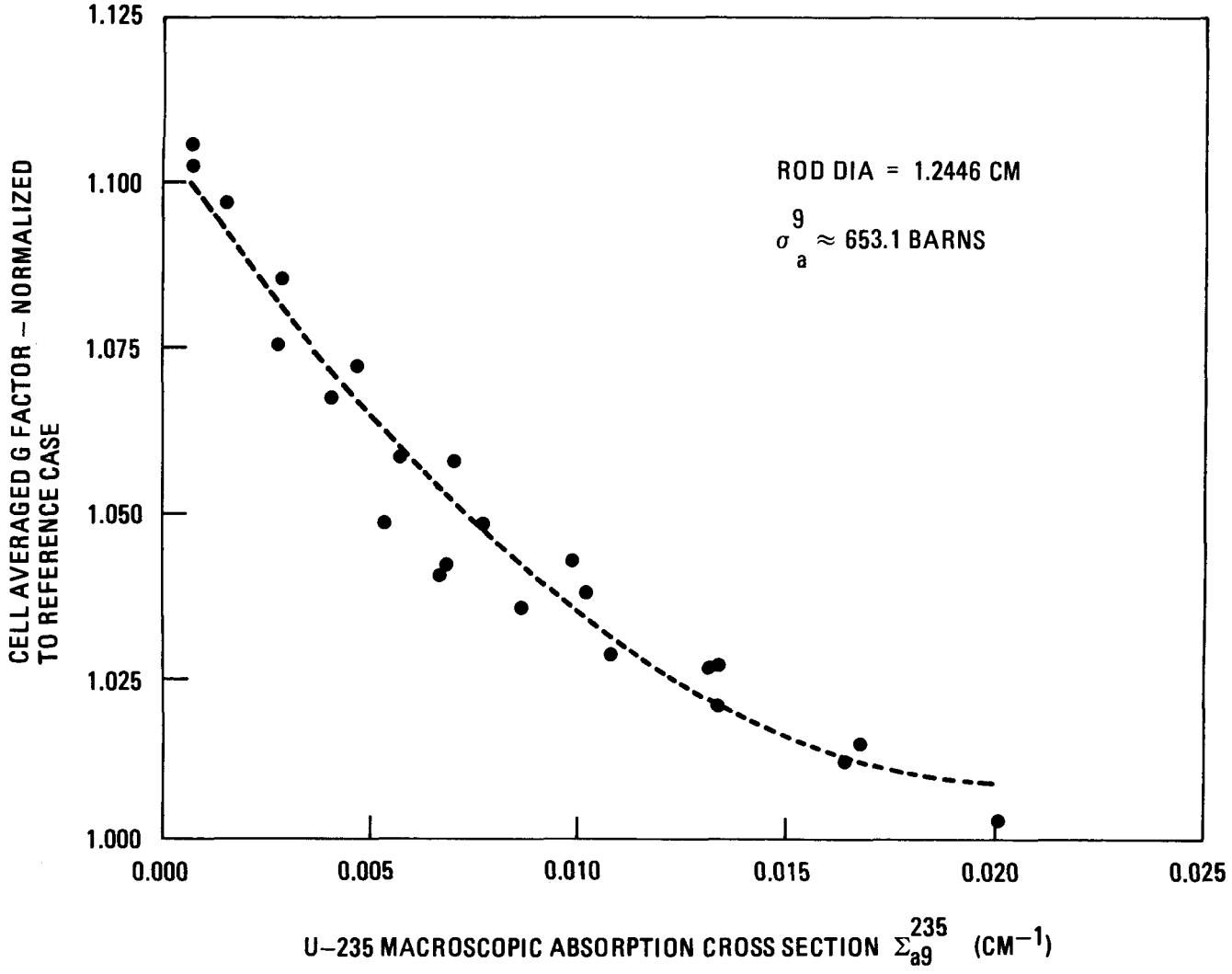

Fig. 15 U-235 self-shielding factor - GARGOYLE Group 9

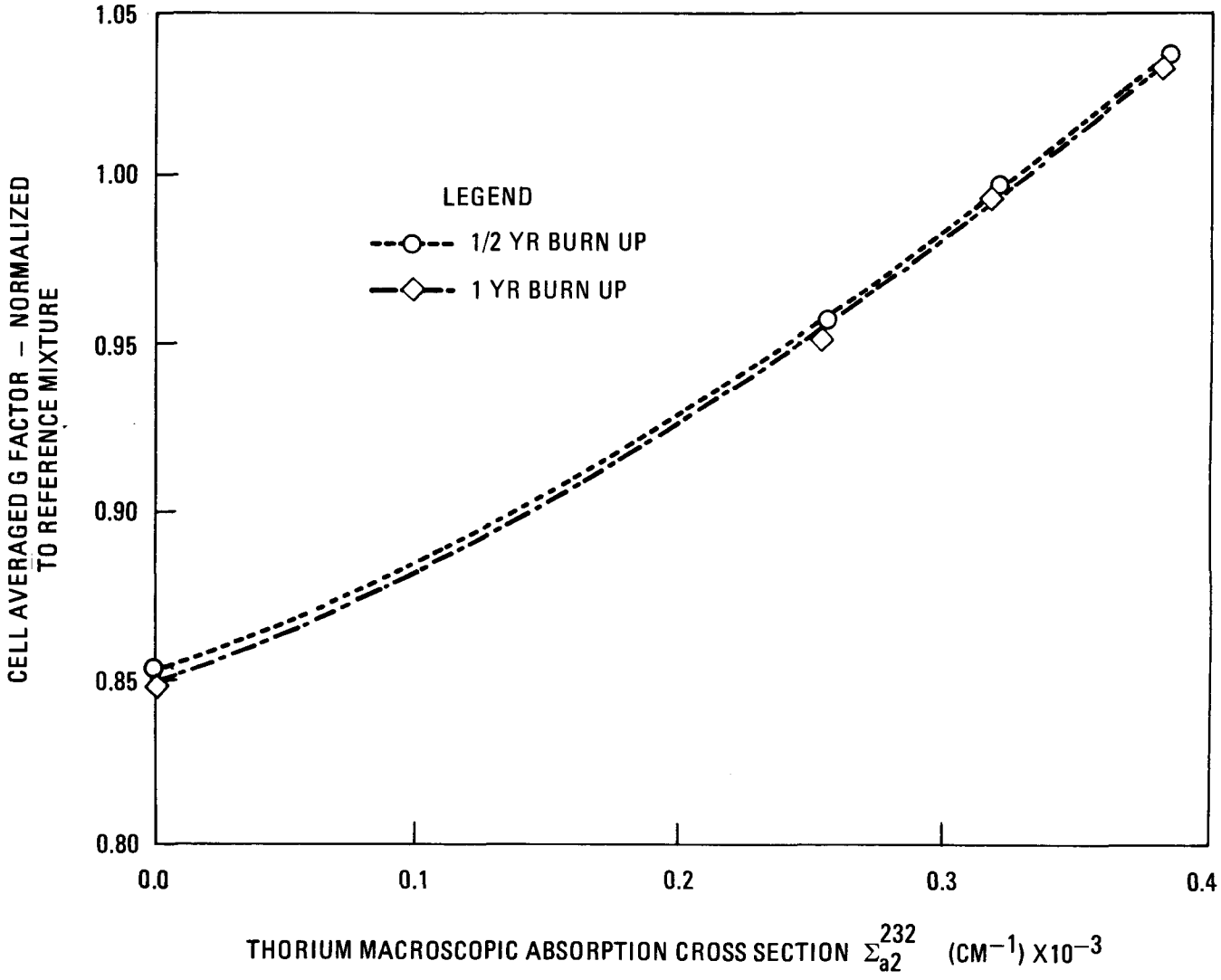

Fig. 16 Th-232 self-shielding factor - GAUGE Group 2

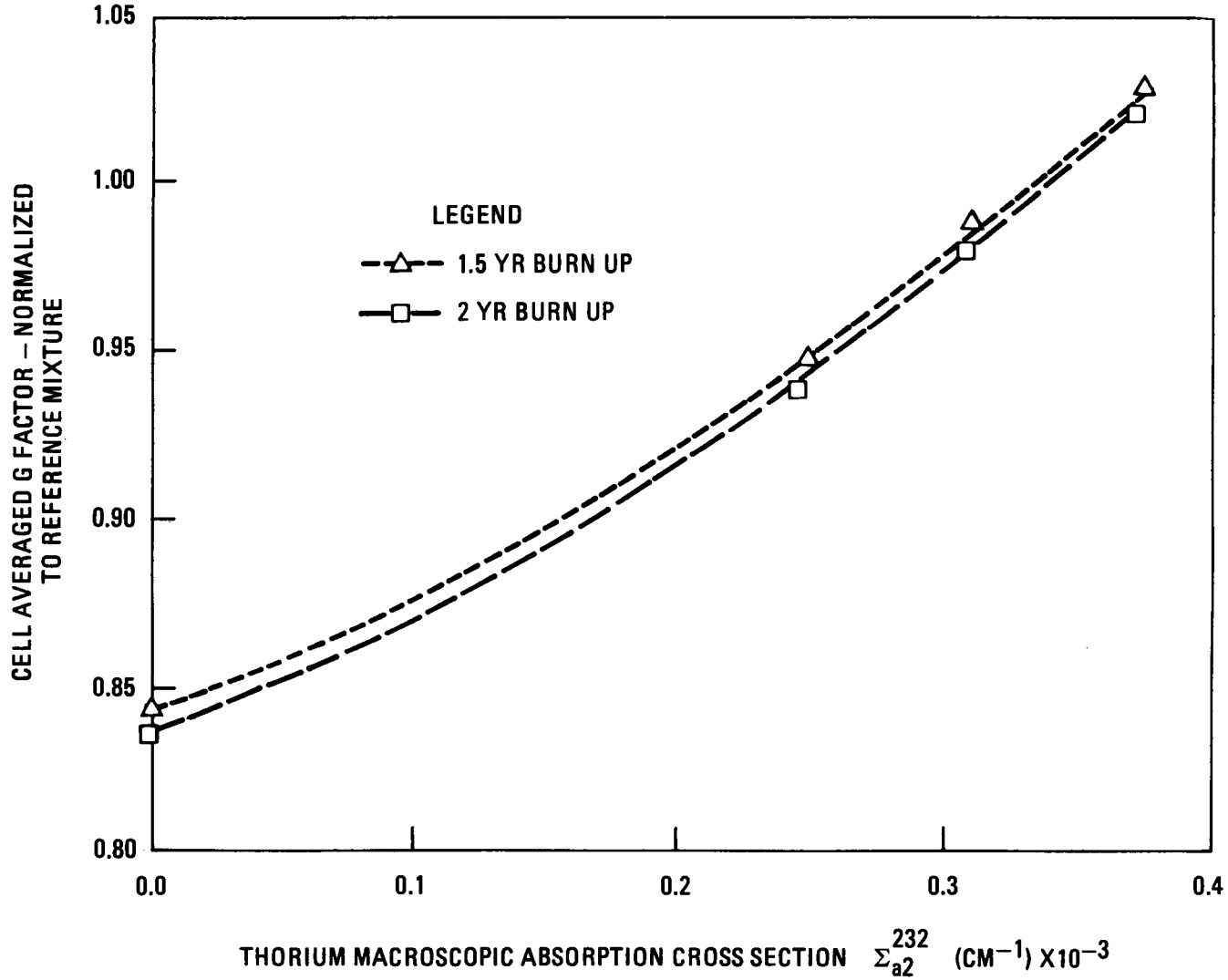

Fig. 17 Th-232 self-shielding factor - GAUGE Group 2

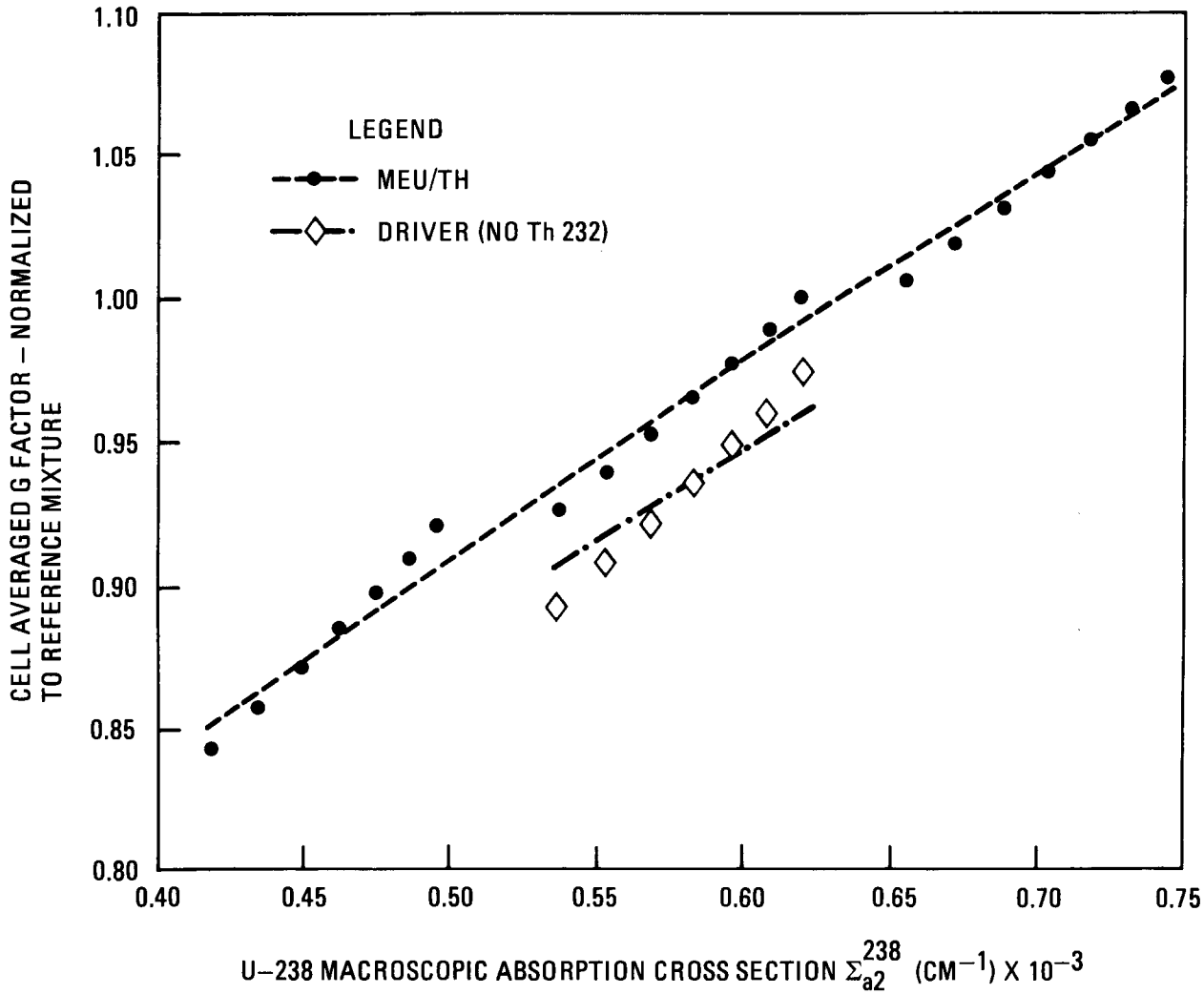

Fig. 18 U-238 self-shielding factor - GAUGE Group 2

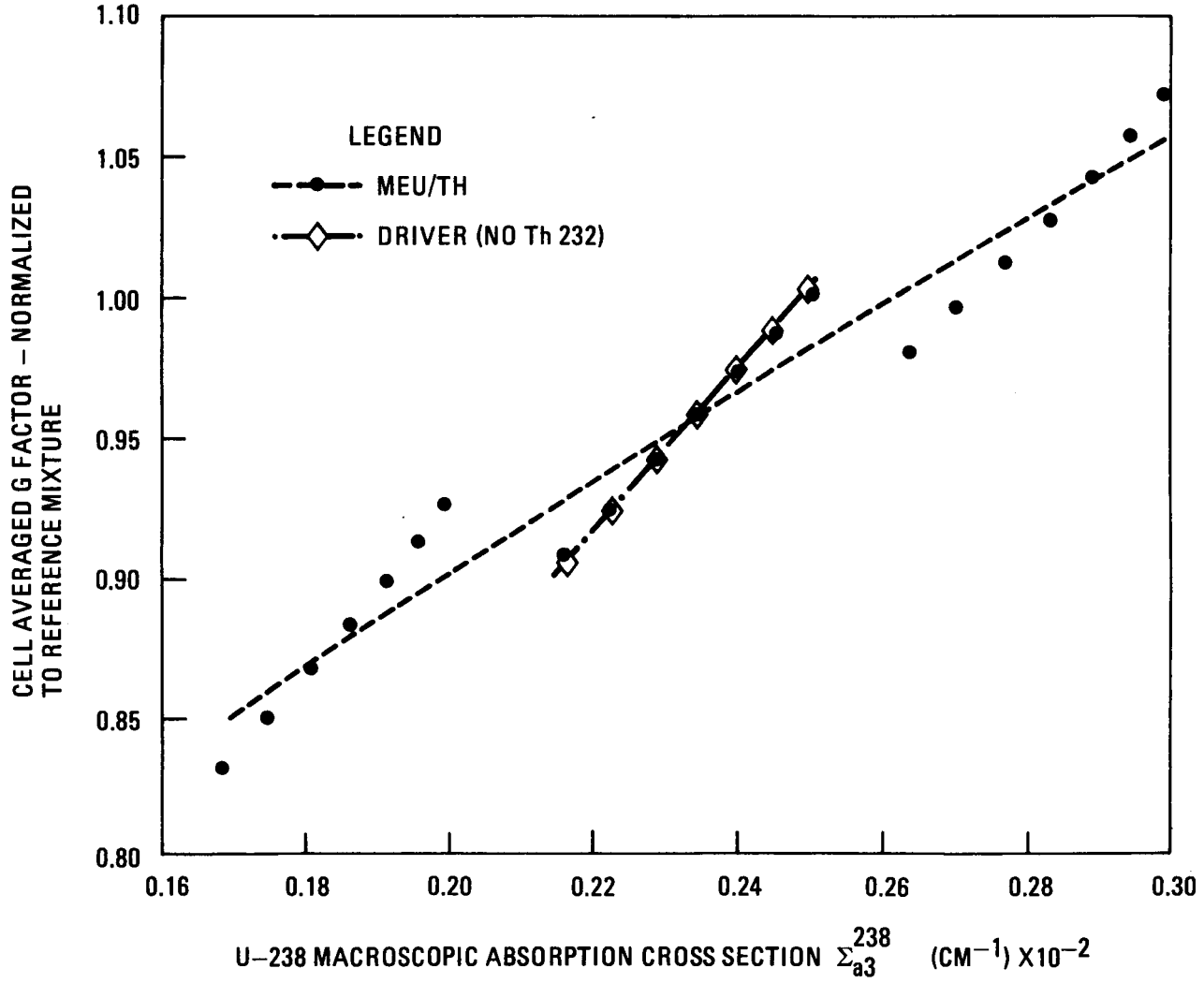

Fig. 19 U-238 self-shielding factor - GAUGE Group 3

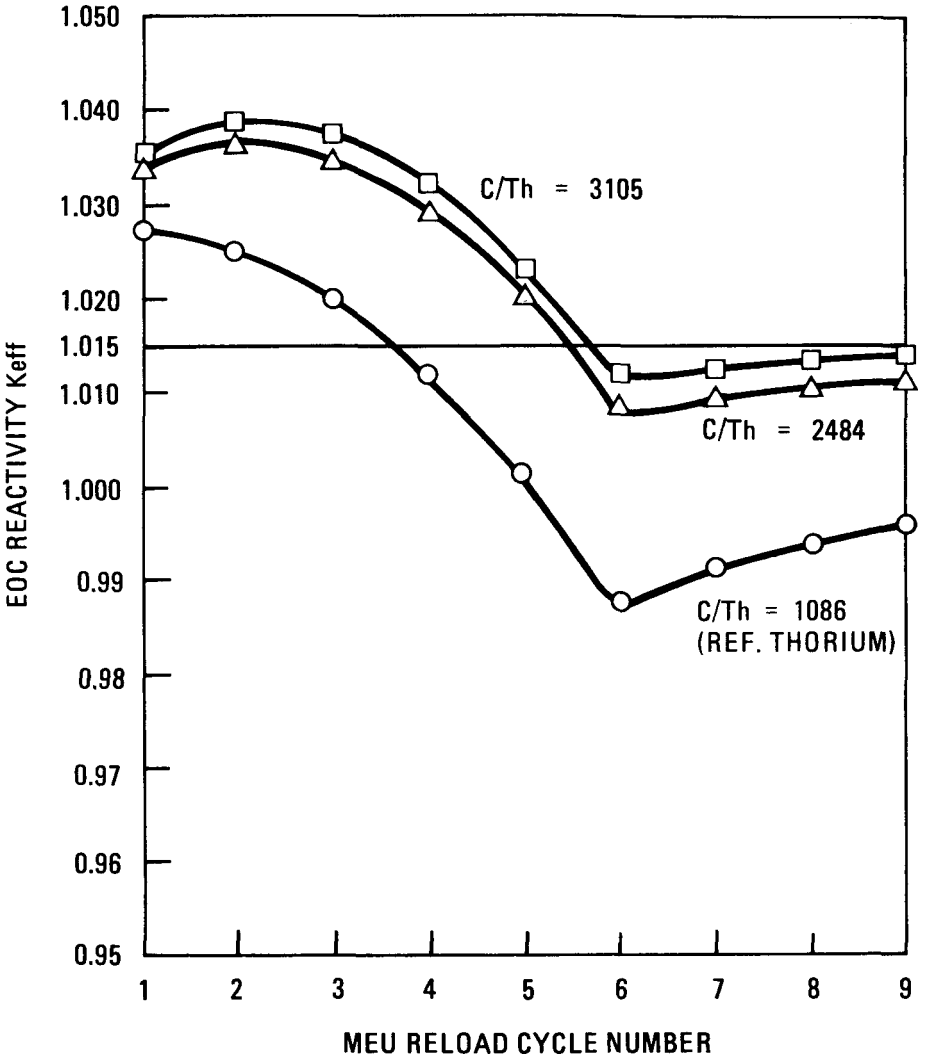

Fig. 20 End-of-cycle reactivity behavior for MEU reloads in the FSV core during transition from HEU fuel cycle as a function of C/Th ratio - C/U = 483.6

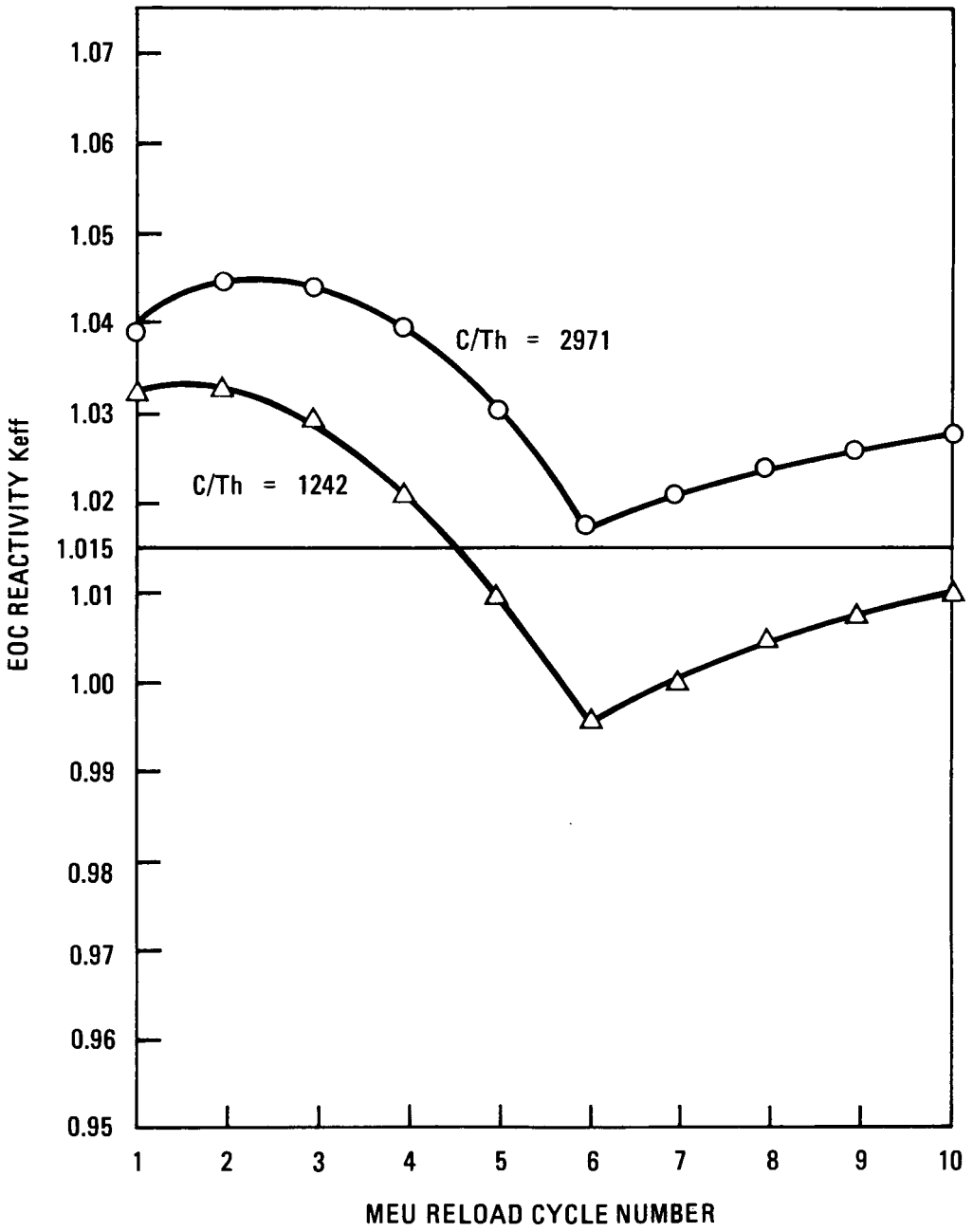

Fig. 21 End-of-cycle reactivity behavior for MEU reloads in the FSV core during transition from HEU operation as a Function of C/Th ratio - C/U = 439.6

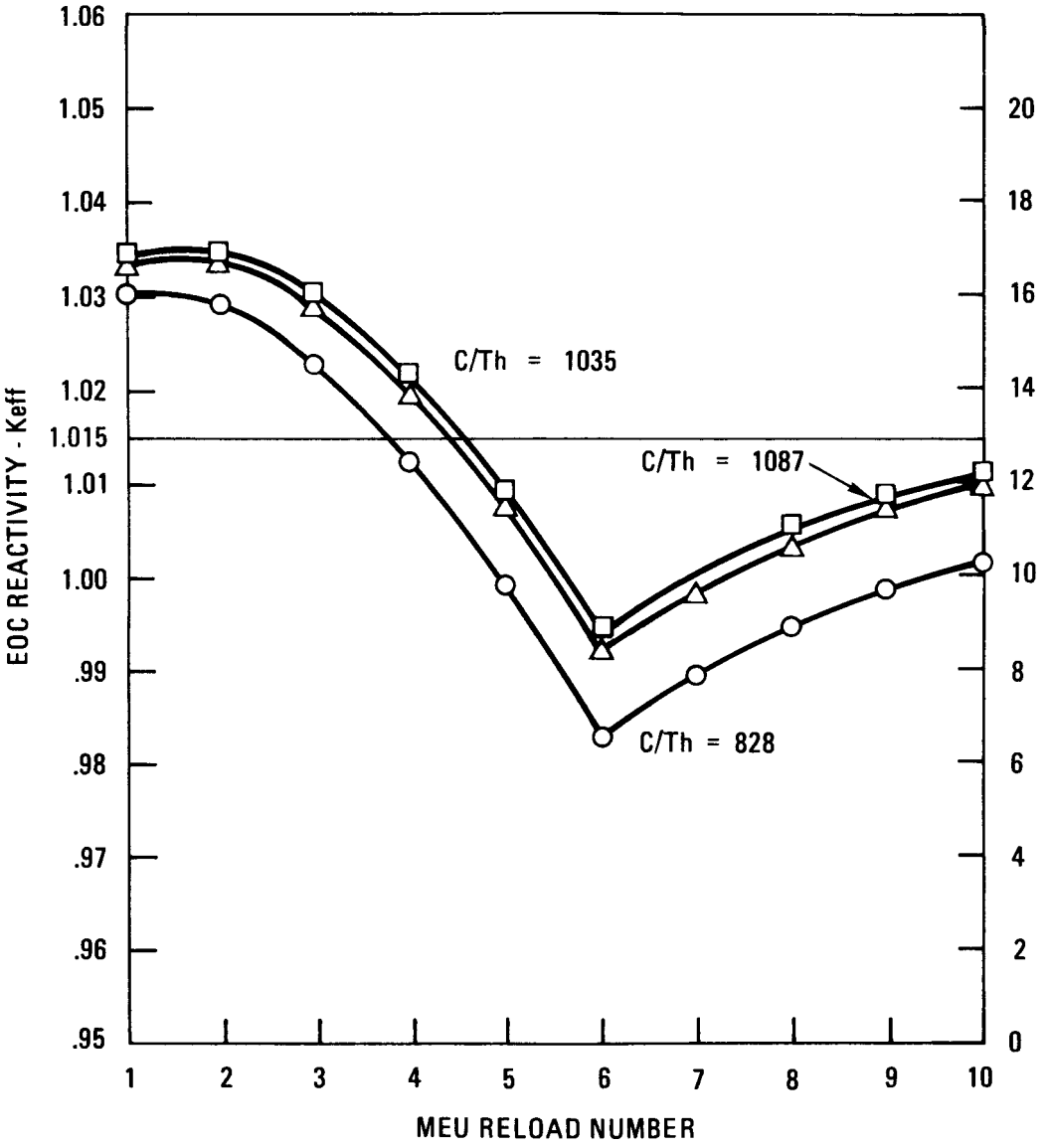

Fig. 22 End-of-cycle reactivity behavior for MEU reloads in the FSV core during transition from HEU operation as a function of C/Th ratio - C/U = 420.5

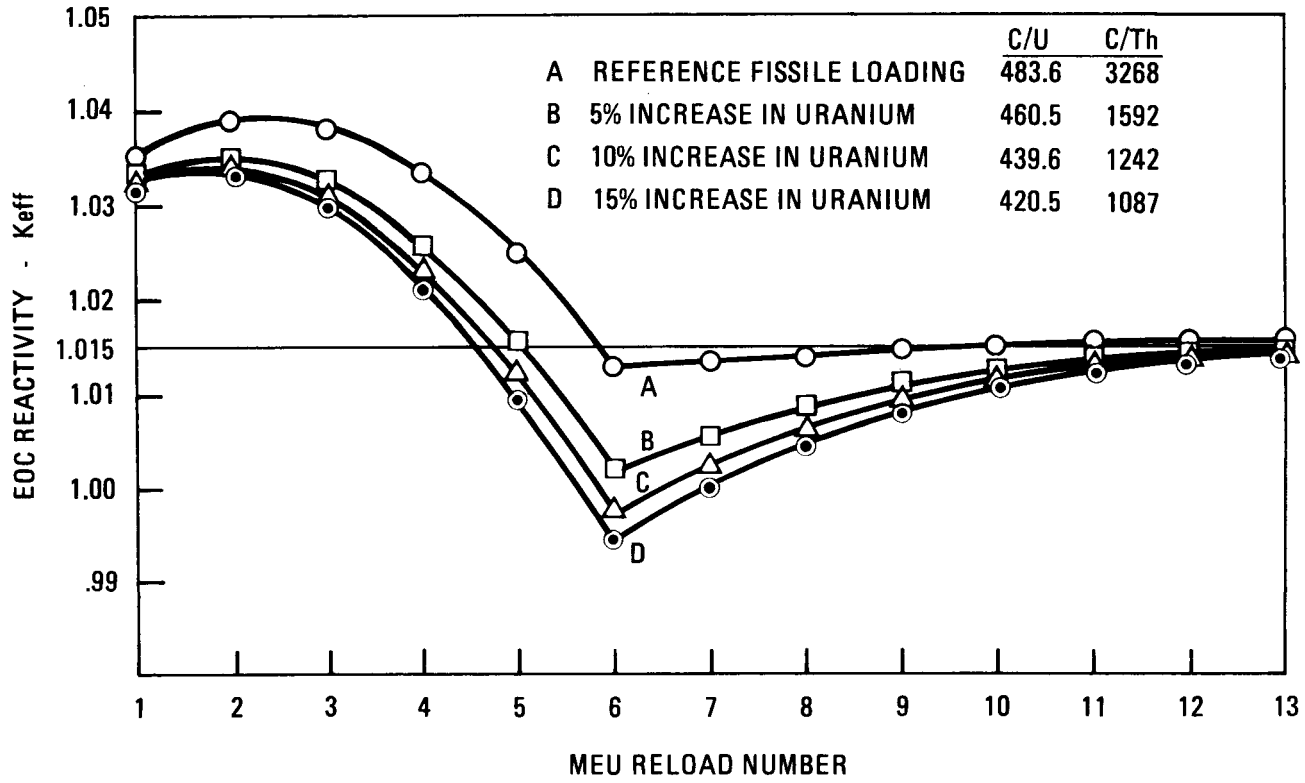

Fig. 23 Thorium loadings necessary to meet end-of-cycle equilibrium cycle reactivity requirements for various fissile loadings

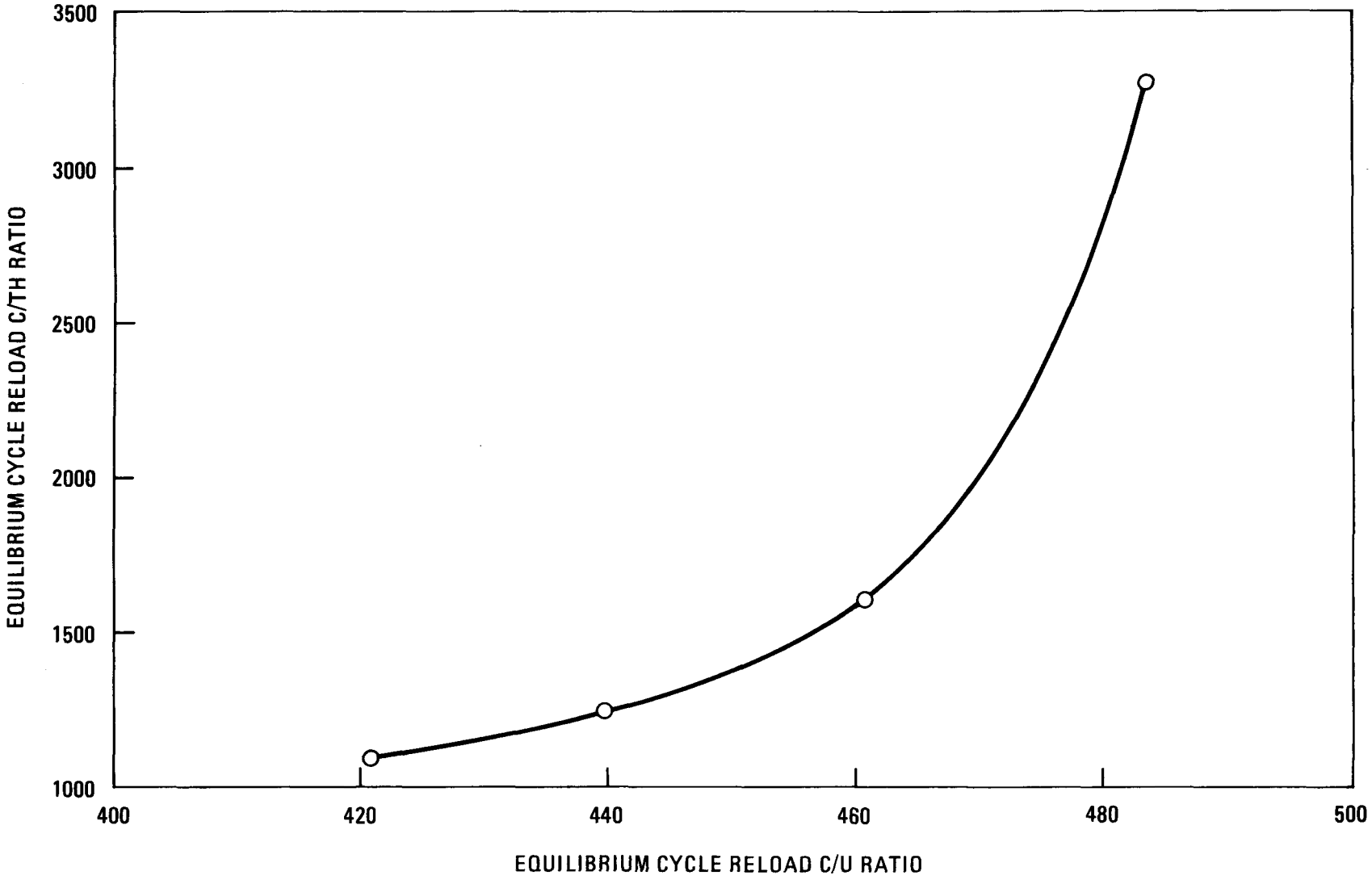

Fig. 24 Equilibrium MEU cycle uranium requirements as a function of C/Th ratio

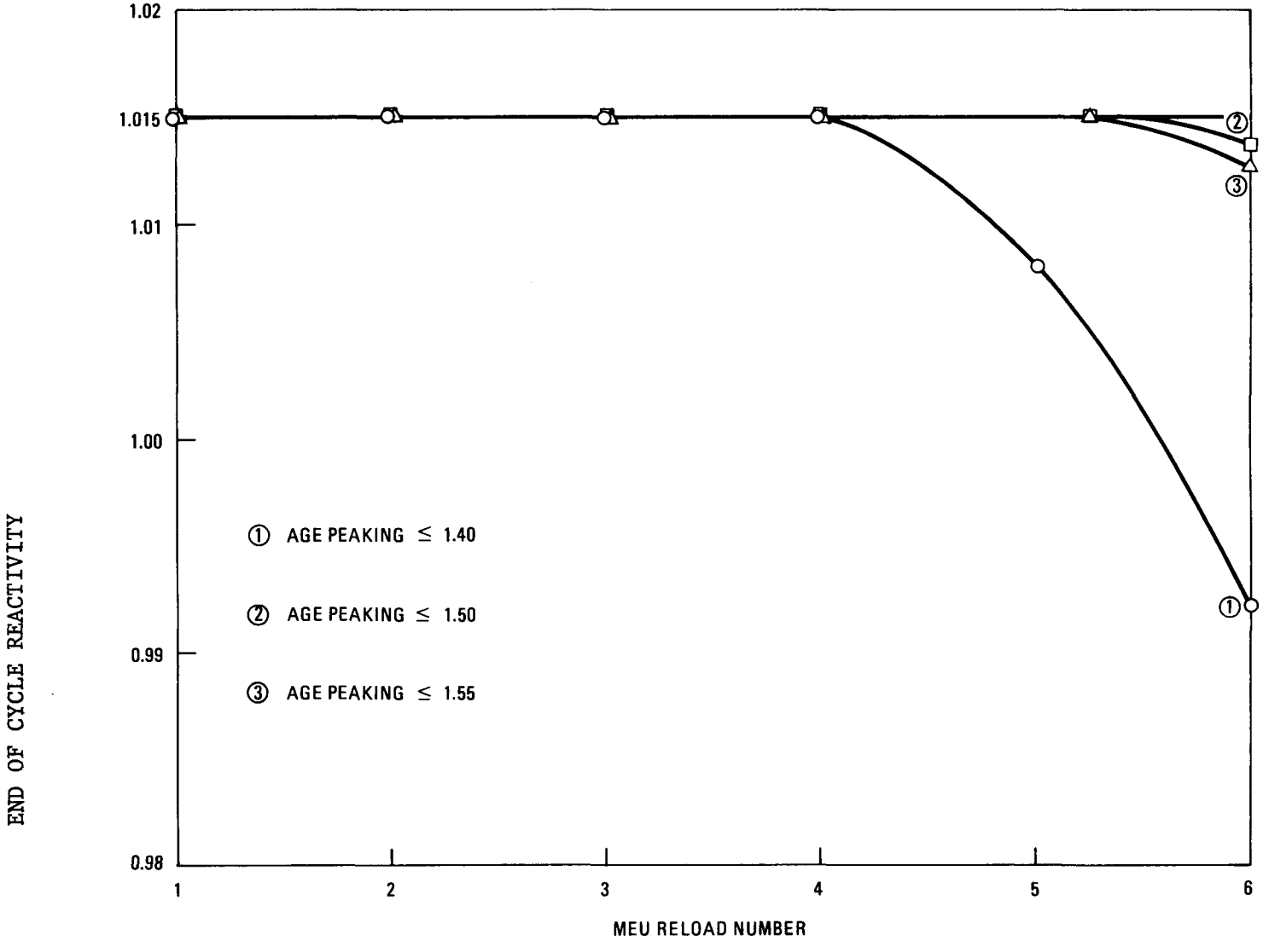

Fig. 25 End-of-cycle reactivity during transition cycles under various APF constraints

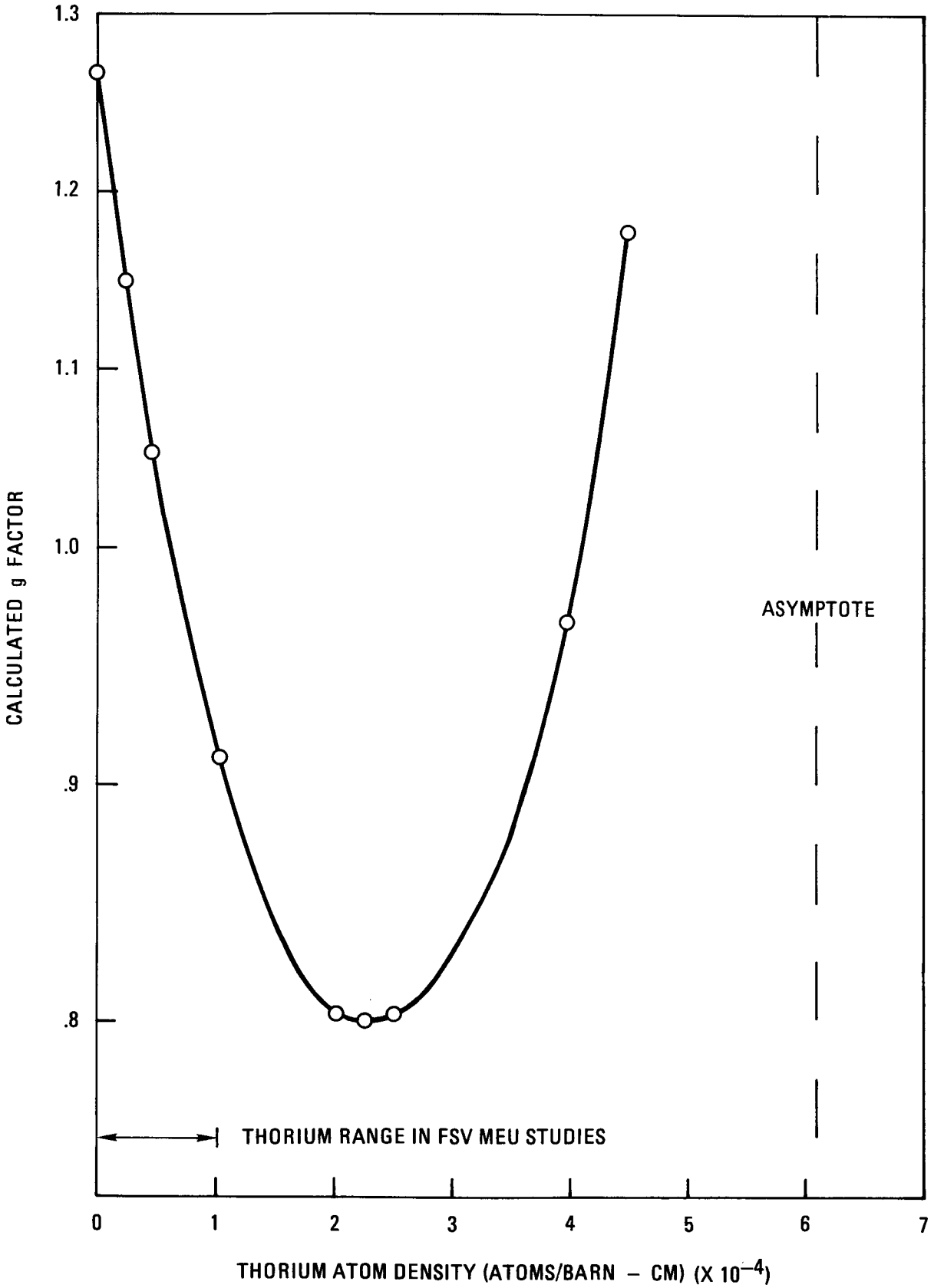

Fig. 26 Typical behavior of the rational self-shielding factor formula for g factors in MEU-HEU fuel transition cases

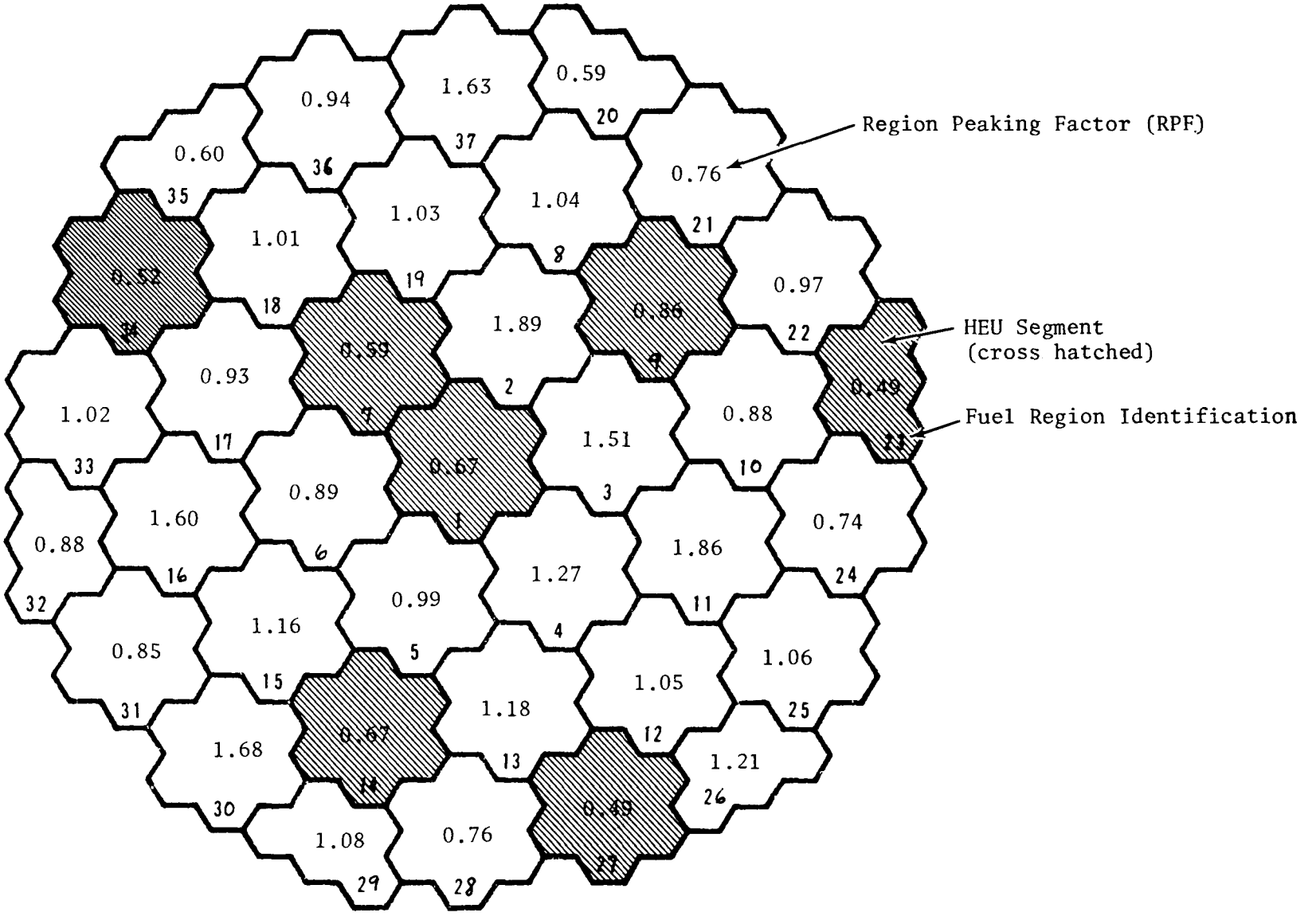

AVERAGE RING POWER

RING	AVG. POWER
0	0.67
1	1.19
2	1.05
3	0.90

Fig. 27 Typical RPF Distribution During Transition Cycle

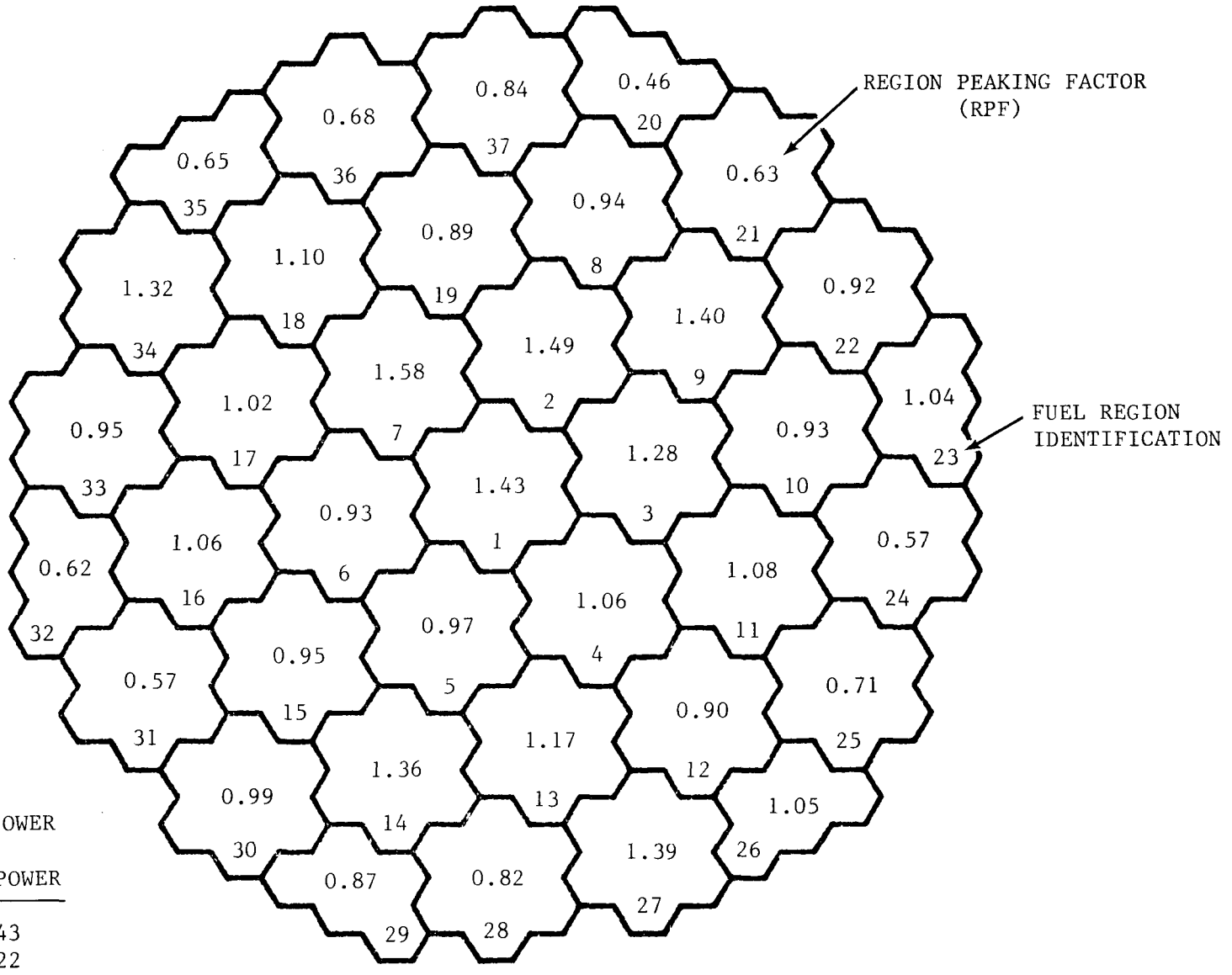

AVERAGE RING POWER

RING	AVG. POWER
0	1.43
1	1.22
2	1.07
3	0.84

Fig. 28 Typical RPF Distribution During Equilibrium Cycles